Contents lists available at ScienceDirect

# Materials Today Bio

journal homepage: www.journals.elsevier.com/materials-today-bio



# Biosynthesis, characterisation and biocompatibility of a unique and elastomeric medium chain-length polyhydroxyalkanoates for kidney glomerular tissue engineering

Syed Mohammad Daniel Syed Mohamed <sup>a,b</sup>, Jack Tuffin <sup>c</sup>, Judy Watson <sup>d</sup>, Andrea Mele <sup>a,b</sup>, Annabelle Fricker <sup>a</sup>, David A. Gregory <sup>a,b,e</sup>, Elbaraa Elghazy <sup>a,f</sup>, Moin A. Saleem <sup>d</sup>, Simon C. Satchell <sup>d</sup>, Gavin I. Welsh <sup>d</sup>, Ipsita Roy <sup>a,b,e,\*</sup>

- <sup>a</sup> School of Chemical, Materials & Biological Engineering, Faculty of Engineering, University of Sheffield, Sheffield, S37HQ, UK
- <sup>b</sup> PHAsT Limited, Sheffield, S1 4DP, UK
- <sup>c</sup> The Discovery Centre (DISC), AstraZeneca PLC, Biomedical Campus, Cambridge, CB2 0AA, UK
- <sup>d</sup> Renal Bristol, Translational Health Sciences, Bristol Medical School, University of Bristol, Bristol, BS1 3NY, UK
- e Insigneo Institute for in silico Medicine, University of Sheffield, UK
- f Department of Construction and Building Engineering, Arab Academy for Science, Technology, and Maritime Transport, Cairo, Egypt

#### ABSTRACT

Polyhydroxyalkanoates (PHAs) are bacteria-derived polymers that are being actively explored for their potential in biomedical engineering applications. These polymers are not only highly biocompatible in nature but also sustainable, produced using renewable substrates, and hence considered future biomaterials. In addition to normal fermentation, PHAs can also be produced through a synthetic biology approach. This study explores a medium chain-length PHA (mcl-PHA) produced by *Pseudomonas mendocina* CH50 by batch fermentation, fed with glucose as the sole carbon source. The polymer was extensively characterised, and it exhibited an elastomeric property of a typical mcl-PHA with  $215 \pm 52$ % elongation at break. The mcl-PHA also had a low melting point,  $T_{\rm m}$ , of around 55 °C, making it processable with various fabrication methods. The extracted mcl-PHA was prepared as a solvent-cast film and tested as a potential cell culture substrate for human glomerular cells, the conditionally immortalised human podocytes (CiHP) and conditionally immortalised human glomerular endothelial cells (CiGEnC). Initial resazurin assay under proliferative conditions showed promising cell metabolic activities of the cells cultured on the mcl-PHA film, comparable with those cultured on tissue culture plastic (TCP). Despite the decreased expression of collagen IV under proliferative conditions, the differentiated co-cultured cells on mcl-PHA had comparable values with cells those grown on TCP. These promising results verified the biocompatibility of the mcl-PHA produced by *P. mendocina* CH50 and established its potential as a bio-based sustainable alternative in biomedical applications including glomerular tissue engineering.

# 1. Introduction

Polyhydroxyalkanoates, widely known as PHAs, are a family of natural sustainable polyesters which are mainly produced by fermentation and synthetic biology approach [1], using aerobic bacteria with many known wild-type or genetically modified strains, including *Pseudomonas* [2]. *Pseudomonas* is one of many Gram-negative bacterial genera with vast potential in producing PHAs due to their versatile metabolic capabilities of converting a range of different carbon sources, including waste materials into PHAs. They mainly produce medium chain-length PHA, or mcl-PHA, with side chains of more than two carbons (Fig. 1) via the phaC1 and phaC2 genes which code for the PHA synthase [3]. They are typically produced intracellularly within the phasin protein envelope in the cytosol of the cells that act as a cellular

carbon reserve [4,5]. These polymers are non-toxic, biodegradable, environmentally friendly, and innately biocompatible; hence they are sought after for their sustainability value and huge range of applications, including in the biomedical area.

Pseudomonas-derived PHAs are currently being actively explored to unlock their massive potential in many applications [2]. Notable species, such as *Pseudomonas putida* [6], *Pseudomonas oleovorans* [7], *Pseudomonas aeruginosa* [8,9], and *Pseudomonas mendocina* [10–12] have been subjected to bioprocess optimisation to determine the best conditions for achieving high yield and productivity of PHAs. Some other lesser-known species, such as *Pseudomonas citronellolis* [13], *Pseudomonas monteilii* [14], *Pseudomonas umsogensis* [15], *Pseudomonas chloroaphis* [16,17], and *Pseudomonas stutzeri* [10,18], to name a few; on the other hand, are also actively being investigated to understand their

<sup>\*</sup> Corresponding author. School of Chemical, Materials & Biological Engineering, Faculty of Engineering, University of Sheffield, Sheffield, S37HQ, UK. *E-mail address*: I.Roy@sheffield.ac.uk (I. Roy).

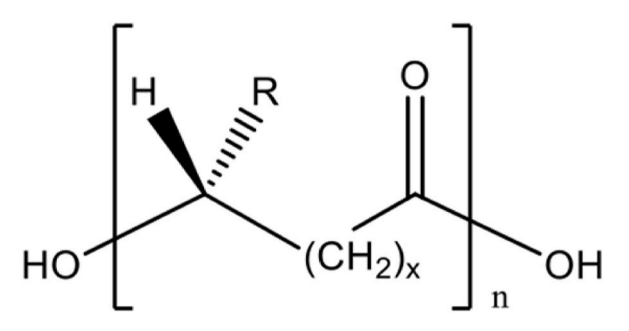


Fig. 1. The general chemical structure of PHAs.

biosynthetic pathways and factors that favour PHA production, including substrate preference, media composition and culture conditions. Furthermore, genetic modification has also been undertaken to introduce and maximise PHA accumulation capability in comparison to wild-type strains, especially using *P. putida* [19].

Due to the robustness of *Pseudomonas* species, there have been attempts to scale up the production of PHAs in order to obtain a higher quantity of the polymer as compared to the conventional shaken-flask. Commonly adopted techniques include batch, fed-batch, and continuous fermentations with a stirred tank bioreactor [2]. For example, a large-scale mcl-PHA production using a 500 L fermentation vessel has been carried out using P. citronellolis DSMZ 50332, fed solely with acetic acid as a batch fermentation. The runs yielded 15.0  $\pm$  0.3 g L $^{-1}$  dry biomass concentration with 3.5  $\pm$  0.5 g  $L^{-1}$  of mcl-PHA concentration from two fermentation runs totalling 1,207 L of working volume [20]. Another upscale attempt to produce mcl-PHA with unsaturated side chains has been carried out using a 100 L bioreactor with a single vessel two-step strategy; step one was batch (Gewürztraminer grape pomace as the substrate in the growth phase), and step two was a fed-batch fermentation (1:1 octanoic acid and 10-undecenoic acid as substrates in the polymer accumulation phase) by P. putida KT2440. This run produced 7.9  $\pm$  0.4 g  $L^{-1}$  final residual biomass, with 5.8 g  $L^{-1}$  of mcl-PHA with a terminal olefin group, simultaneously proving the sustainability in PHA production using waste materials as feedstock in large-scale runs [21]. Another example of successful large-scale fermentation was in a 400 L vessel, using P. putida GPo1, utilising sodium octanoate as a carbon source, which led to the production of poly (3-hydroxyoctanoate) polymer. The fed-batch fermentation led to the production of 17.8  $\pm$  0.3 g L<sup>-1</sup> cell dry mass at the end of the fermentation, with 48.0  $\pm$  2.6 % of polymer content [22].

P. mendocina has also been utilised as a potential PHA producer and is gaining significant attention in sustainable biopolymer production using renewable carbon sources [23,24]. Mcl-PHA, for instance, can be produced from sugar, especially glucose, which P. mendocina strains can use to undergo fatty acid de novo synthesis and hence to promote the elongation of the PHA side chain [25]. However, there are few reports describing a scaled-up fermentation using P. mendocina; most describe shaken-flask experiments. A study using P. mendocina PSU cultivation utilising biodiesel liquid waste led to the production of a high polymer content of PHA, up to 77 % dry cell weight (dcw) of mcl-PHA from 3.7 g  $L^{-1}$  dry cell mass in shaken 250 ml Erlenmeyer flasks [12]. Using a similar cultivation technique but with P. mendocina strain 0806, culturing with glucose led to the production of around 2.1 g  $L^{-1}$  of dcw with less polymer content, only 32 % dcw [26]. Another batch of shaken-flask culture using P. mendocina CH50, using sodium octanoate, led to the production of poly(3-hydroxyoctanoate). 0.6 g L<sup>-1</sup> dcw was obtained at the end of the fermentation after 54 h, with 22.5 % dcw of polymer content [27]. Using this strain, a relatively larger scale of fermentation was carried out in a 20 L stirred tank bioreactor, unravelling the potential of scaled-up PHA production using *P. mendocina*. The run used coconut oil as a sustainable carbon source, producing a terpolymer of mcl-PHA with up to 58 % dcw polymer content with 2.5 g  ${\rm L}^{-1}$  of biomass concentration after 48 h of fermentation [11]. The selection of sustainable carbon sources, as mentioned, indeed confirmed the green nature of PHA production using *P. mendocina* strains in producing PHA, not limited to conventional shaken-flask techniques but also scaled-up production using bioreactors with larger fermentation volume.

In addition, *P. mendocina* NK-01 has been extensively subjected to metabolic engineering to enhance the accumulation of PHAs, including inhibition of  $\beta$ -oxidation by deleting six genes involved in this process, leading to the increased mcl-PHAs titre by 10 folds. Deletion of the *phaZ* gene also led to the preservation of the dominant monomer of mcl-PHA by avoiding depolymerisation [28]. In addition, morphology engineering has been carried out to promote cell elongation by knocking out the cell fission ring gene, *minCD*, allowing the cells to accumulate higher PHA content [29].

PHAs are known to be versatile for many applications and interest in using them in the pharmaceutical and biomedical sectors is increasing. They are known for their biocompatibility with mammalian cells; hence, cell and tissue engineering research has showcased PHAs as prospective materials replacing synthetic ones. For P. mendocina, only PHAs produced by the P. mendocina strain CH50 has been reported to demonstrate biocompatibility for tissue engineering applications. One of the studies reported that the mcl-PHA produced by, P. mendocina, promoted neuronal cell attachment and proliferation, 40 % higher than standard tissue culture plastic [11]. Meanwhile, other work validated the biocompatibility of surface-coated mcl-PHA with polydopamine by in vivo subcutaneous implantation in a rat model, which after four weeks post-implantation displayed no inflammatory response and exhibited tissue integration with the promotion of neovascularisation compared to uncoated samples [30]. PHAs also have potential in delivering active compounds for therapeutic purposes, such as injectable microspheres using a type of mcl-PHA, poly(3-hydroxybutyrate-co-3-hydroxyvalerate-co-3-hydroxyhexanoate), in delivering neurogenic drugs [31,32] for androgenetic alopecia treatment [33], and delivering bone morphogenetic protein (BMP) to promote directed osteogenic differentiation of human bone marrow mesenchymal cells (hBMSCs) [34].

This study aimed to study the production of mcl-PHA by *P. mendocina* CH50 using a scaled-up batch fermentation of 10 L working volume, utilising glucose as the sole carbon source, and eventually testing its biocompatibility, for the first time, using glomerular cells, for future kidney tissue engineering representing a soft tissue engineering application. The polymer produced was thoroughly characterised to obtain information regarding its chemical, thermal and mechanical properties. Later, the resulting polymer was explored for its suitability for kidney tissue engineering using two types of unique renal cells, conditionally immortalised human glomerular cells; podocytes [35] and endothelial cells [36]. This study confirmed, for the first time, the potential of the mcl-PHA produced using *P. mendocina* CH50, in kidney tissue engineering and for an *in vitro* 3D kidney model development.

# 2. Materials and methods

All chemicals were purchased from Merck (Sigma-Aldrich) (Darmstadt, Germany), VWR International (Pennsylvania, USA), Lonza (Basel, Switzerland) and Thermo Fisher Scientific (Massachusetts, USA).

The setup for the fermentation used in this study was a 15 L jacketed single-wall bioreactor vessel equipped with a dual Rushton turbine with constant stirring at 574 rpm. Temperature, pH, dissolved oxygen tension and stirring were monitored and regulated in real-time using Applikon Biotechnology Z310110011 EZ Control Bioreactor (Delft, The Netherlands). All equipment for the cultivation was purchased from Getinge (Derby, UK).

# 2.1. Polymer production and preparation

The P. mendocina strain CH50 was used as the producer of the PHA. It

was activated before inoculation using a two-stage shaken flask growth: nutrient broth as the first stage and mineral salt media as the second stage, as established [11,27,37–40]. The bioreactor fermentation run utilised 10 L of fermentation working volume, with 20 g  $\rm L^{-1}$  of glucose as a sole carbon source in a batch mode for 48 h [11].

Temperature, pH and dissolved oxygen tension were acquired continuously in real-time throughout the fermentation by the bioreactor control. The cell density was measured by optical density at 600 nm *via* sampling. The temporal sampling provided information regarding temporal biomass concentration and other information for the temporal profile, including residual nitrogen concentration by phenol nitroprusside-sodium hypochlorite method [41] and glucose assay by 3, 5-dinitrosalisylic acid (DNS) reagent to detect reducing sugar from the supernatant [42].

The polymer was extracted using the two-step Soxhlet extraction by placing the freeze-dried biomass in a paper thimble: the first step used methanol to wash dissolvable lipid and protein impurities, and the second was chloroform extraction. The polymer was later precipitated using cold methanol under stirred conditions, collected and dried until constant weight was obtained. The solvent-cast film was produced by dissolving the polymer into chloroform to obtain a 10 % w/v solution and pouring it into a glass petri dish to be dried under a fume hood at room temperature [11].

#### 2.2. Polymer characterisation

The chemical structure of the polymer was identified by proton nuclear magnetic resonance (<sup>1</sup>H NMR) spectroscopy using Bruker AVIII 400 MHz "Marmaduke" 5 mm solution state double resonance broadband probes. Functional group validation has been carried out by Fourier-Transform Infrared-Attenuated Total Reflection (FTIR-ATR) spectroscopy using a Perkin Elmer Frontier FT-IR spectrometer by putting a solid sample on a diamond probe.

For polymer quantification, the gas chromatography (GC) method was used. The biomass samples were subjected to methanolysis to extract and methanolyse the polymer into quantifiable monomeric components. Standard curves were used using the relevant commercial 3-hydroxy methyl esters [43,44]. This was used to determine the polymer content, polymer titre, and polymer productivity in correspondence with other temporal data.

Further monomer determination was carried out using the gas chromatography-mass spectroscopy (GC-MS) method by Agilent 7200 Accurate Mass Q-ToF GC-MS, using the same samples from the methanolysis. The detected peaks are analysed and compared with the National Institute of Science and Technology (NIST) database, depending on the matching factor.

Thermal characteristics of the polymer were determined with the Differential Scanning Calorimetry (DSC) method using the Perkin Elmer DSC4000 instrument to detect the glass transition ( $T_{\rm g}$ ) and melting ( $T_{\rm m}$ ) temperatures by scanning the sample at 20 °C per minute. Meanwhile, the degradation temperature ( $T_{\rm d}$ ) was obtained with thermogravimetric analysis (TGA) using the Perkin Elmer Pyris 1 TGA instrument with a similar scan rate.

Molecular weight quantification was conducted using the gel permeation chromatography (GPC) method with Viscotek GPCmax VE2001 GPC solvent/sample module equipped with PLgel 5  $\mu m$  Mixed C heated in a Gilson column oven with a column set length of 650 mm, and Waters 410 Differential Refractometer as the Differential Refractive Index detector with an injection volume of 100  $\mu L$ . Peaks were detected using Cirrus software, set for manual analysis. The values were calculated against the polystyrene 9-point standard curve with the equation as follows:

$$y = 16.8 - 1.73x + 0.0895x^2 - 0.00208x^3$$

Where y is the molecular weight,  $M_w$ , and x is the retention time in

minutes, using narrow standard calibration with a curve fit of three. This analysis was conducted at the Department of Chemistry, University of Sheffield.

The bulk mechanical property of the polymer was measured using a MultiTest-dV Motorised force tester (Mecmesin) instrument with a 25 N load cell. Pre-cut polymer films into a dog-bone shape following the ISO standard ASTM D638 Type V, and were loaded between two vertical metal grips. Five similar samples were used as replicates.

### 2.3. Cell work and cytocompatibility

Bristol Renal, University of Bristol, has developed the two conditionally immortalised human glomerular cell lines used for this study [35,36]. Conditionally immortalised human podocytes (CiHP) were maintained using RPMI-1640 media with the addition of insulin-transferrin-selenium (ITS) solution to make up 1 % v/v and foetal bovine serum (FBS) to make up 10 % v/v [35]. Conditionally immortalised glomerular endothelial cells (CiGEnC) were maintained using EBMTM-2 basal medium (CC-3156) equipped with EGMTM-2 MV Microvascular Endothelial Cell Growth Medium SingleQuots<sup>TM</sup> supplements (CC-4147) [36]. CiHP was transduced to overexpress green fluorescent protein (GFP-actin), and mCherry-actin for CiGEnC [45]. Both cell types were incubated at 33 °C for proliferation for seven days and switched to 37  $^{\circ}\text{C}$  to arrest cell division and start cell differentiation for 14 days. The viability assay used a resazurin assay over seven days under proliferative conditions at 33 °C. A 10 % v/v solution of 1 mM sodium resazurin salt was prepared with culture media. The media was removed and resazurin solution was introduced to the cell culture and incubated for 4 h before being read using a plate reader for fluorescence, using a 530-570 nm excitation wavelength and 585-590 nm emission wavelength [46]. All cell cultures used 10,000 cells per mL as the seeding density in 96-well plates with 200  $\mu L$  working volume per well.

#### 2.3.1. Staining and imaging

Initially, all cell culture samples are fixed using 4 % methanol-free formaldehyde for 15 min. The formaldehyde is then removed and immediately they were blocked using a blocking buffer consisting of 5 % normal serum and 0.3 % Triton<sup>TM</sup> X-100 in phosphate buffer saline for an hour. Next, antibody staining was introduced, using 0.5 % of the primary antibody solution Invitrogen Collagen IV Monoclonal Antibody (1042) (1:200 dilution), eBioscience<sup>TM</sup> to stain collagen, with 1 % normal serum and 0.3 % Triton<sup>TM</sup> X-100 in phosphate buffer saline, and let incubated overnight at 4 °C. After that, 4  $\mu$ M of 4′,6-diamidino-2-phenylindole or DAPI staining as nuclei stain was introduced into the cells for 15 min. All images were acquired using Zeiss LSM880 Airyscan Confocal utilising a Z-stack setting and processed using Fiji Image J software, scanning 0.7 mm² area for at least three locations on a sample to acquire information for mean fluorescent intensity and number of cells.

The neat polymer underwent Scanning Electron Microscopy (SEM) analysis to assess its surface qualitatively. The samples were coated with gold using a Quorum Q150RSplus instrument, resulting in a gold deposition thickness of 5 nm. Image capture was performed using an FEI Inspect F microscope, a general-purpose Field Emission Gun–Scanning Electron Microscope (FEG-SEM) equipped with Secondary Electron (SE) and Backscattered Electron (BE) image detectors, as well as Energy Dispersive Spectrometry (EDS). The SEM facility is at Sorby Centre, University of Sheffield.

# 2.3.2. Statistical analysis

All analyses were done using two-way ANOVA statistical analysis using Šídák's multiple comparisons test by comparing the data from mcl-PHA to TCP, through GraphPad Prism software.

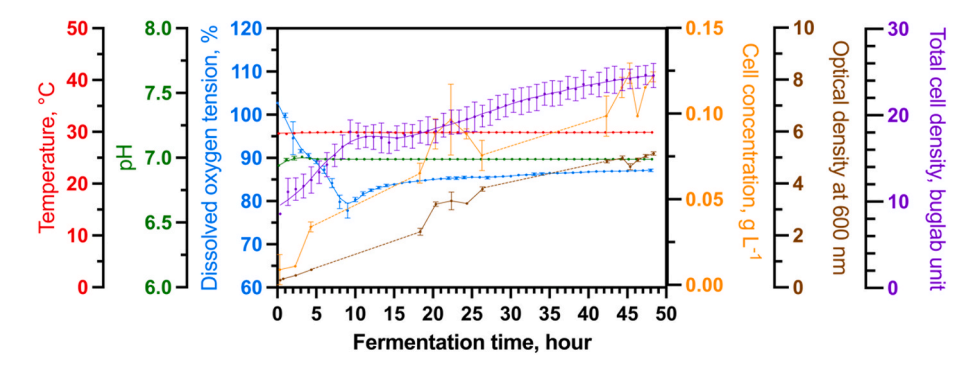
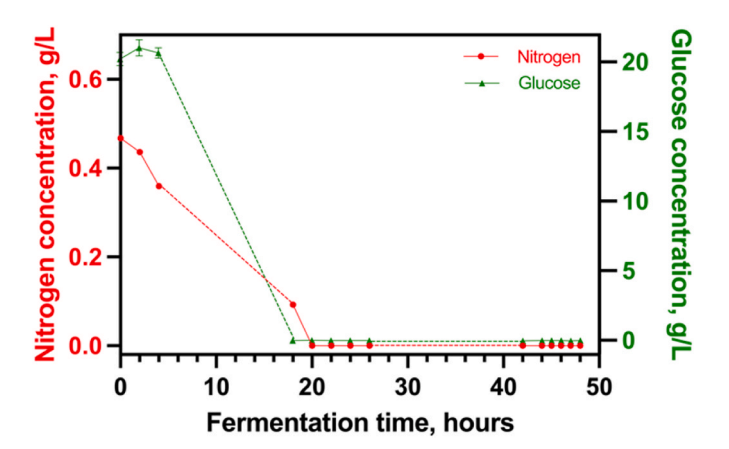
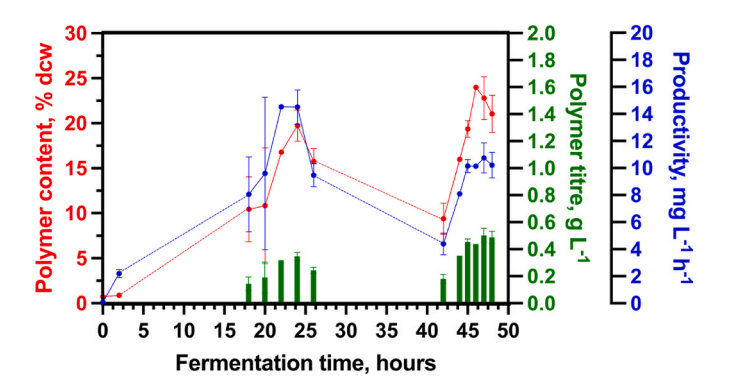


Fig. 2. Fermentation profile for mcl-PHA production by *P. mendocina* CH50 using glucose. Temperature, pH, and dissolved oxygen tension were acquired in real-time. Cell concentration and optical density were acquired at selected time points by manual samplings; each point is n = 2, with gaps (*dotted lines*) between 4–18 h and 26–42 h due to out-of-hours access limitations. All error bars are standard deviations.



**Fig. 3.** Temporal nitrogen (red curve) and glucose (green curve) residue estimation plots of *P. mendocina* CH50 using glucose. Each point is n=4 with error bars representing standard deviation, with gaps (*dotted lines*) between 4–18 and 26–42 h due to out-of-hour access limitations.



**Fig. 4.** Temporal polymer content of % dry cell weight (dcw) (red), polymer titre (green), productivity (blue) plots of *P. mendocina* CH50 using glucose. Each point is n=2 with an error bar representing standard deviation, with gaps (*dotted lines*) between 4–18 and 26–42 h due to out-of-hour access limitations.

#### 3. Results and discussion

#### 3.1. Production of mcl-PHA by P. mendocina CH50

*P. mendocina* CH50 has been selected to produce the mcl-PHA in this study. It was fed by glucose for over 48 h of fermentation, conducted with temporal monitoring to understand the growth pattern. The abiotic temporal parameters in the fermentation included the temperature, pH,

and percentage of dissolved oxygen tension.

The temperature and pH of the 15 L bioreactor with 10 L working volume were stable throughout the fermentation, respectively, at 29.99  $\pm$  0.05 °C and pH 6.99  $\pm$  0.01. The fermentation had a high oxygen level throughout, starting with almost 100 % dissolved oxygen tension and gradually decreasing to 77.8  $\pm$  2.3 % after 9 h. The oxygen level was eventually maintained until the end of the fermentation, indicating that the bacterial culture was maintained at a certain level of growth. Unlike a similar fermentation utilising coconut oil as the sole carbon source, in which the run experienced an abrupt decrease of oxygen level from 100 % to around 0 % within the first hour [11], the run from this study was in oxygen-sufficient conditions, maintained at 80.4  $\pm$  0.5 % (minimum value observed) and 87.1  $\pm$  0.3 % (maximum value observed), introduced by a balance of stirring speed and air inflow rate. The cell concentration also increased over time, reaching a maximum of  $2.3\pm0.1$  g  $L^{-1}$  at the 45th hour. The optical density increased, and the highest reading of 25.6  $\pm$  1.4 was observed at the end of fermentation at the 48th hour (Fig. 2).

The nitrogen component is a limiting factor in this study. Despite this run being conducted in batch mode, a restrictive amount of 0.5 g L $^{-1}$  of ammonium sulphate was introduced. This gradually decreased and reached a plateau at 18 h at a value lesser than 0.1 g L $^{-1}$  and remained so until the end of fermentation (Fig. 3). This observation slightly differs from the previous studies; one that used coconut oil observed a plateau of the nitrogen concentration after 27 h [11], and another study using glucose and fructose as the carbon source observed the plateau after around 12–13 h [47]. This plateauing occurs when the limited supply of nitrogen available in the media has been used up during the run in supporting the growth of the bacteria and no further growth can hence occur in the absence of nitrogen.

Meanwhile, glucose consumption was intensive during the first 20 h of the run. When the glucose began to get depleted, less oxygen was consumed, indicating a lack of growth of the bacteria. This is consistent with the increment of the oxygen concentration after 10 h (Figs. 2 and 3). The fed-batch run producing mcl-PHA using *P. putida* IPT 046 is the most similar fermentation in which a complete glucose depletion was observed around 12–15 h of fermentation similar to the 18 h observed in this work [47].

For information regarding the temporal polymer production, hourly samples were taken and subjected to methanolysis. Methanolysed samples were then eventually subjected to gas chromatography analysis, and data acquired were used to calculate the polymer content, titre, and productivity.

The initial maximum polymer content was observed around halfway through the fermentation run, at 22 h, with a 10.8 % dry cell weight (dcw) content corresponding with the polymer titre value of around 0.23 g  $\rm L^{-1}$ . However, the highest polymer titre was observed at around 46 h with a value of around 0.24 g  $\rm L^{-1}$  and 9.2 % dcw of polymer content. These parameters experienced a slight decrease at the end of the

**Table 1**Yield parameters for mcl-PHA production by *P. mendocina* CH50 at 48 h.

Yield	Parameters	Values		
Cell yield	Cell mass per volume of fermentation broth	$\begin{array}{c} 2.31 \pm 0.05 \ \text{g} \\ \text{L}^{-1} \end{array}$		
Polymer yield	Polymer percentage in the context of dry cell weight (dcw)	$\begin{array}{l} 21.03\pm2.08~\%\\ \text{dcw} \end{array}$		
	Polymer per unit mass of dry cell weight	$0.37 \pm 0.03 \text{ g} \\ \text{g}^{-1}$		
	Polymer per unit mass of substrate	$\begin{array}{l} {\bf 24.38\pm2.27mg} \\ {\bf g}^{-1} \end{array}$		
Titre	Polymer per volume of fermentation broth	$\begin{array}{l} 0.49 \pm 0.05 \; \text{g} \\ L^{-1} \end{array}$		
Productivity	Polymer per volume of fermentation broth per unit of fermentation time	$\begin{array}{c} 10.16 \pm 0.95 \; mg \\ L^{-1} \; h^{-1} \end{array}$		

fermentation with values around 8.7 % dcw and 0.22 g L $^{-1}$  titre. Meanwhile, the polymer productivity trend was consistent with the polymer content and titre. It peaked at 22 h with around 10.5 mg L $^{-1}$  h $^{-1}$ . As time progressed, the productivity decreased, with a value of only around 4.6 mg L $^{-1}$  h $^{-1}$  at the end of the fermentation. Overall, the fermentation experienced polymer production fluctuation trends, with a sharp increment between 15 and 22 h, a decrease afterwards, and an increase between 40 and 46 h, slightly decreasing until the end of the run (Fig. 4). Ultimately, at the end of the fermentation, the mcl-PHA produced exhibited a polymer titre of 0.49  $\pm$  0.05 g L $^{-1}$  and 10.16  $\pm$ 

 $0.95 \text{ mg L}^{-1} \text{ h}^{-1} \text{ productivity (Table 1)}.$ 

The fermentation process was carried out in batch mode. PHAproducing bacteria are well-known to accumulate PHA under nutrientlimiting conditions, such as when carbon, nitrogen, or phosphorus sources become scarce. These stresses trigger the biosynthesis of PHA as an intracellular energy reserve to support survival during periods of starvation [48]. Although detailed reports specifically documenting this behaviour are limited, it can often be inferred indirectly through key indicators. In this study, for example, the depletion of nitrogen and glucose at approximately the 20 h (Fig. 3) coincided with a noticeable increase in PHA accumulation over the subsequent 5 h window (Fig. 4). However, this upward trend gradually reversed over the next 16 h, likely due to the bacteria metabolising the stored PHA to sustain themselves. While this trend has not been extensively described in literature, Basnett et al. observed a comparable pattern with a similar bacterial strain cultured using coconut oil, where nitrogen depletion around 27 h triggered a 20 % increase in PHA accumulation [49]. This fermentation run was especially distinctive due to the unexpected increase of PHA accumulation around the 42 h point, marked by a further 15 % increase over the following few hours (Fig. 4). This increase could be due to a second phase of PHA accumulation after the bacterial growth reached a high value of cell concentration of around 0.125 g  $L^{-1}$  as seen in Fig. 2.

This fermentation run successfully produced mcl-PHA from glucose by utilising *P. mendocina* CH50, with a promising yield of 0.49  $\pm$  0.05 g  $\rm L^{-1}$  for batch fermentation within a 10 L working volume bioreactor.

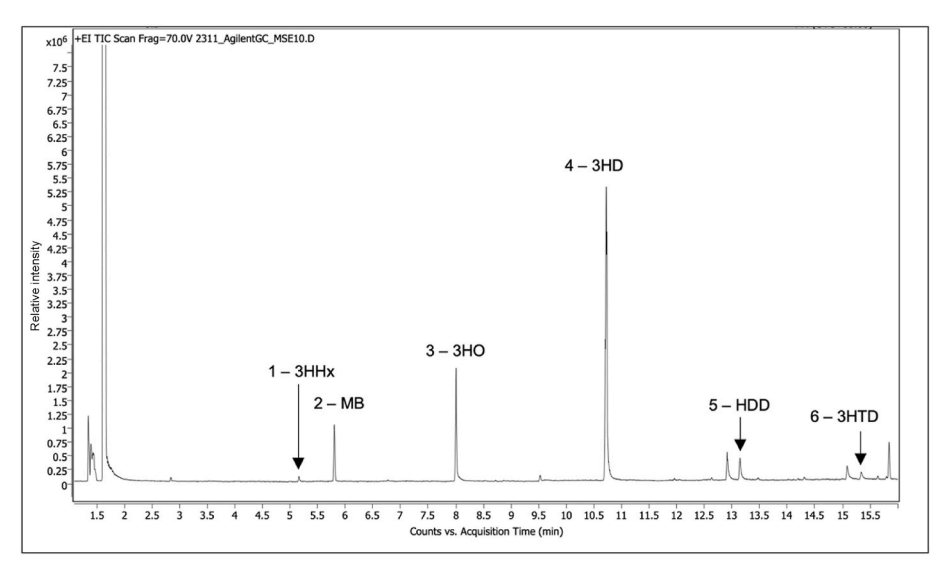


Fig. 5. GC-MS chromatogram detecting 3-hydroxymethyl ester monomers from mcl-PHA produced by P. mendocina CH50 when fed with glucose.

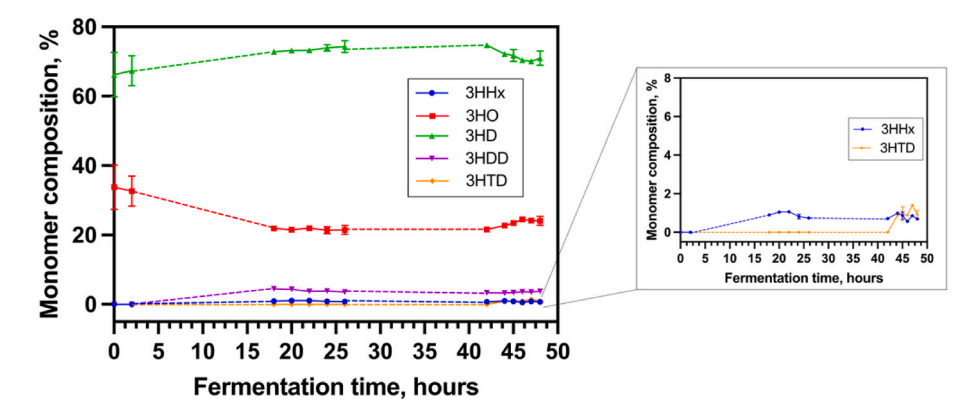


Fig. 6. Monomer composition in terms of molar percentage across the fermentation run for 3HO, 3HD, and 3HDD in the main graph and 3HHx and 3HTD in the inset graph. The 3HD composed most of the monomer with 71.5 mol% of the polymer.

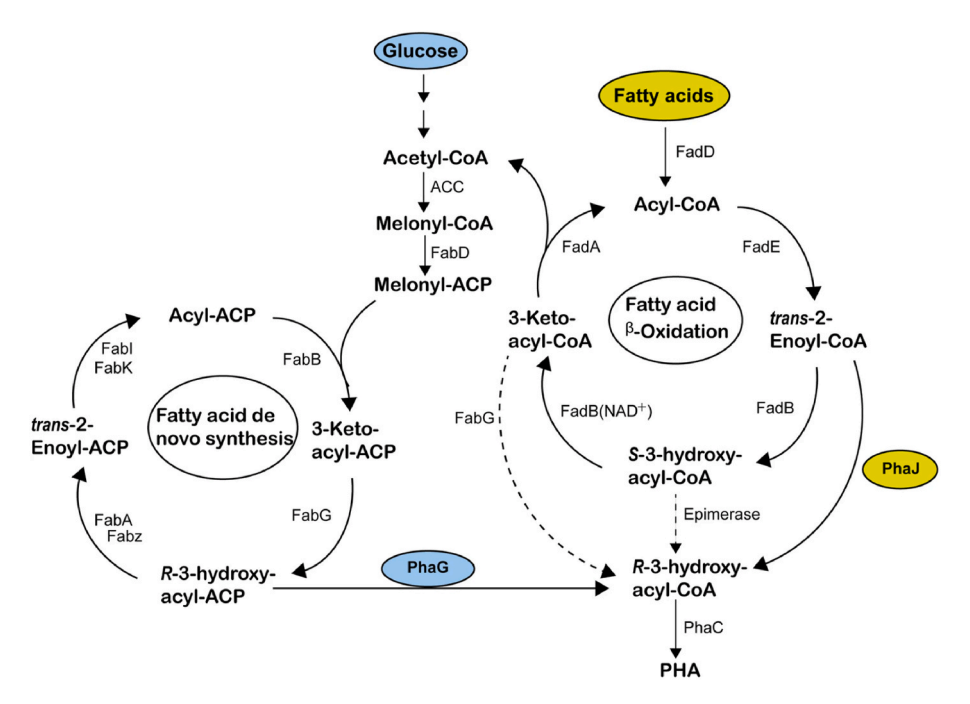


Fig. 7. General PHA synthesis pathways from glucose and fatty acids in bacteria. Adapted from Liu et al., licensed under a Creative Commons Attribution 4.0 [53].

Adopting a fed-batch fermentation strategy in the future, further enabling the potential of optimising and eventually increasing productivity, could further improve the yield.

#### 3.2. Characterisation of mcl-PHA by P. mendocina CH50

#### 3.2.1. Monomer confirmation

The polymer produced by *P. mendocina* CH50 was subjected to GCMS to validate the monomer composition of the mcl-PHA. Five different monomer methyl esters were detected from the analysis, namely 3-hydroxyhexanoate (3HHx), 3-hydroxyoctanoate (3HO) 3-hydroxydecanoate (3HD), 3-hydroxydodecanoate (3HDD), and 3-hydroxytetradecanoate (3HTD) (Fig. 5). The MS spectra compare the signal from the corresponding component's sample and the NIST database. All MS spectra showed the presence of m/z=103 signal, the total molecular weight of the hydroxyl group,  $\alpha$  and  $\beta$  carbon, and the ester bond as the main component for 3-hydroxyalkanoate esters (Fig. 5) [18, 501.

The temporal variation of the monomer percentage was quantified using the GC method by considering the flame ionisation detector (FID) signal to obtain the mole percentage. Initially, there were no 3HHx, 3HDD, or 3HTD detected from the samples within the first 4 h of the fermentation. However, 3HHx and 3HDD monomers were detected later at 18 h of fermentation, and the 3HTD monomer only appeared after 44 h. The highest monomer content was 3HD, averaging 71.5  $\pm$  2.4 mol%, followed by 3HO with 24.4  $\pm$  3.6 mol% throughout the fermentation, making the polymer principally a medium chain-length PHA or mcl-PHA (Fig. 6). The temporal variation in the monomer content of the PHA reflects the temporal variation in the substrate pool available to the PHA synthase enzyme during the biosynthesis of the polymer. To the best of our knowledge, this is the first time such an in-depth study has been carried out with respect to the temporal variation of the monomer content of the PHA. In future this can be exploited to produce mcl-PHA of bespoke monomer content and hence, with related specific material properties.

The utilisation of glucose in producing PHA is common, given its renewable nature. In PHA-producing bacteria, several pathways related to sugar metabolism, especially glucose, promote the biosynthesis of the bio-polyester. The product may differ due to the metabolic capacity of

the bacterial strain. For both short chain-length or medium chain-length PHA biosynthesis, glucose is first subjected to glycolysis to produce two pyruvate molecules and later converted *via* pyruvate oxidation into acetyl-CoA, a significant precursor of most cellular metabolic pathways, including PHA biosynthesis. Lu et al. reviewed possible 3-hydroxyalkyl-CoA monomers produced to produce scl-PHA, such as 3-hydroxybutyryl-CoA for P(3HB) production, 3-hydroxyvaleryl-CoA for P(3HV), and 4-hydroxybutyryl-CoA for P(4HB) [51], the polymerisation of which ultimately takes place by the action of the enzyme PHA synthase [52]. For mcl-PHA biosynthesis, the acetyl-CoA would be introduced into specific pathways to elongate the side chain, known as dissociated fatty acid biosynthesis, or *de novo* fatty acid synthesis, or *de novo* lipogenesis, to produce 3-hydroxyacyl-ACP, which later would undergo transesterification to produce 3-hydroxyacyl-CoA for PHA biosynthesis by the relevant PHA synthase (Fig. 7) [25,51,53].

P. mendocina is known to produce mcl-PHA, especially when fed with fatty acids [11,12]; limited reports mentioned glucose as a carbon source [24]. This study confirmed that P. mendocina, specifically strain CH50, can biosynthesise mcl-PHA from glucose by undergoing de novo lipogenesis, which is consistent with assessment of the production of 3-hydroxyacyl-ACP and eventually 3-hydroxyacyl-CoA in the PHA biosynthetic pathways by Kroumova et al. [23] One study reported that P. mendocina NK-01 produced mcl-PHA from glucose with mcl-monomers including 3HO and a significantly higher 3HD monomer composition [54], comparable to the result from this study. Similar to a study using P. mendocina 0806, the fermentation that utilised glucose produced a higher 3HD composition and was tailorable up to 97–99 mol% when the media had a carbon:nitrogen (C:N) ratio of >40, and around 80 mol% for <40 [24,55].

The monomer composition of the mcl-PHA produced from this study is not widely reported, and is hence novel; only one study demonstrated a similar monomer composition of the mcl-PHA produced using *P. stutzeri* 1317 using glucose as substrate, with a monomer content of 2.4 mol% for 3HHx, 21.3 mol% for 3HO, 63.2 mol% for 3HD, 4.2 mol% for 3HDD, and 1.0 mol% for 3HTD, having lower 3HD content compared to this study [18]. It is also worth mentioning that a study produced mcl-PHA from *P. mendocina* NK-01 grown using glucose as the carbon source, including an 18-carbon monomer of 3HOD (3-hydroxyoctadecanoate); 17.8 mol% for 3HO, a higher content of 3HD with

 Table 2

 Monomer composition, mol% comparison with studies with P. mendocina using different substrates and other Pseudomonas sp. using glucose as substrate.

Bacterial (Substrate)	Monomer composition, mol%								Ref.
	ЗНВ	3HV	ЗННх	ЗНО	3HD	3HDD	3HTD	C=Ca	
P. mendocina strains on different substrate									
P. mendocina CH50 (glucose)	-	-	0.7	24.4	71.5	3.1	0.4	_	This study
P. mendocina CH50 (coconut oil)	-	-	_	30.4	48.4	21.2	_	-	[11]
P. mendocina CH50 (sodium octanoate)	_	_	-	100.0	_	_	_	-	[27]
P. mendocina CH50 (biodiesel waste)	-	-	2.3	27.8	55.7	14.2	_	_	[38]
P. mendocina CH50 (sodium gluconate)	-	-	_	~20	~70	~10	_	_	[23]
P. mendocina PSU (biodiesel liquid waste)	~85	-	_	~10	~5	_	_	_	[12]
P. mendocina 0806 (glucose)	-	-	5	17	71	1	_	_	[24]
Pseudomonas on glucose as substrate									
P. stutzeri 1317 (glucose)	-	-	2.4	21.3	63.2	4.2	1.0	_	[18]
P. aeruginosa ATCC 9027 (glucose)	-	-	_	_	74.4	15.2	_	_	[59]
P. guezennei CNCM-I-3358 (glucose)	-	-	1.0	24.0	66.0		7.0	4.0	[60]

 $<sup>^{</sup>a}$  C=C = unsaturated side chain.

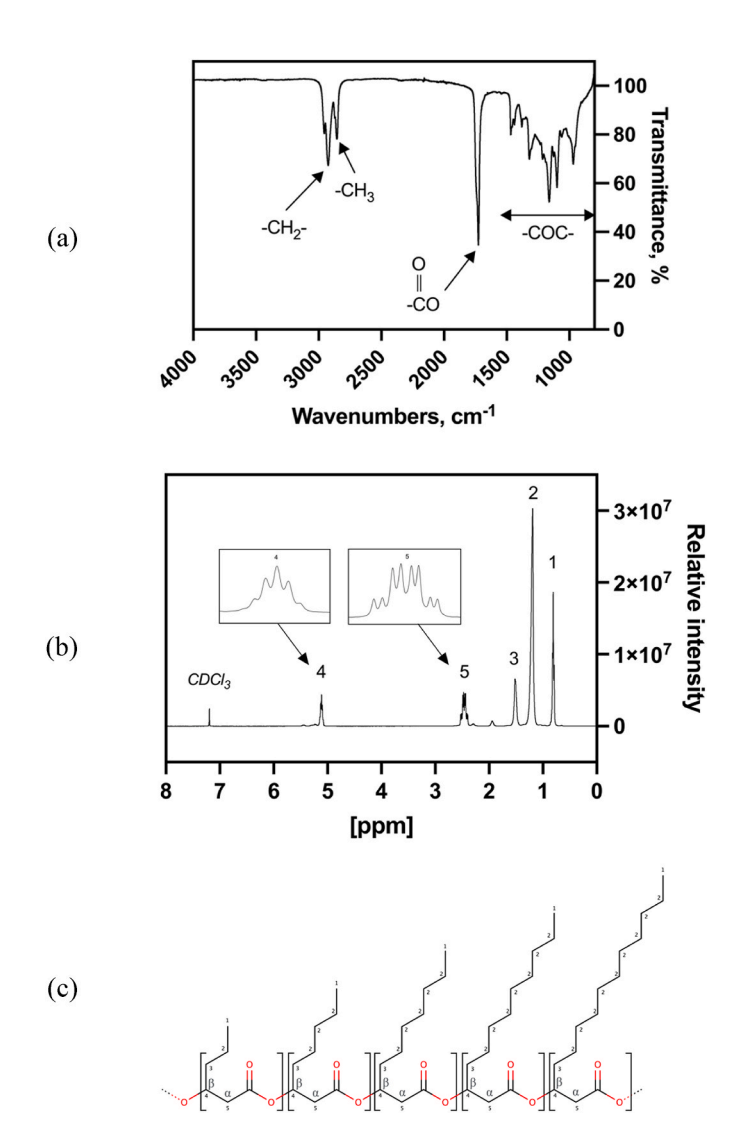


Fig. 8. (a) FTIR spectrum, and (b)  $^1\mathrm{H}$  NMR spectrum, and (c) proposed molecular structure for mcl-PHA produced by *Pseudomonas mendocina* CH50.

73.1 mol%, and the rest totalling of 9.2 mol% consists of 3HHx, 3HDD, 3HTD, 3HHxD, and including the 3HOD monomers, with no specified percentage mentioned [56]. Meanwhile, *P. mendocina* CH50 grown with coconut oil as the main carbon source, produced P(3HO-co-3HD-co-3HDD) with 30.4  $\pm$  2.1 mol%, 48.4  $\pm$  0.8 mol% and 21.2  $\pm$  2.0 mol%, respectively (Table 2) [11]. Other *Pseudomonas* sp. that produce

mcl-PHAs are mainly grown on fatty acid and oil and can also produce unsaturated side chains, which are attractive for chemical functionalisation [57]; they are abundant within the repertoire of academia and are also industrially attractive [2,58].

As mentioned, Pseudomonas sp. generally yielded mcl-PHAs when fed with fatty acids due to the process of fatty acid β-oxidation. Meanwhile, when sugar, such as glucose was used as the carbon source, they undergo fatty acid de novo synthesis when chain elongation occurs, resulting in longer side chains as in a typical mcl-PHA (Fig. 7). Between different P. mendocina strains, is the main consistency is that they all produce mcl-PHAs regardless of using sugar or fatty acid as a carbon source, as displayed in Table 2. The monomer composition was widely known to be affected by the type of carbon source; however, the duration of the fermentation was hypothesised to play an important role here. For instance, for glucose-fed strains, P. stutzeri 1317 was run for 48 h [18], similar to P. mendocina CH50 from this study; both yielded similar monomer types. Meanwhile, P. mendocina 0806 had the same fermentation duration, which resulted in almost similar monomers, apart from the absence of 3HTD [24]. On the other hand, P. aeruginosa ATCC 9027 and P. guezennei CNCM-I-3358 had significantly different compositions, though also fed with glucose, both cultivated only for 8 h [59,60].

#### 3.2.2. Molecular structure

The structure of the mcl-PHA was further validated using Fourier-Transform Infrared (FTIR) spectroscopy and proton nuclear magnetic resonance (<sup>1</sup>H NMR) spectroscopy.

The key functional group on the polymer produced by the *P. mendocina* CH50 was detected through FTIR analysis. The side chain terminal methyl group -CH $_3$  is detected as the alkane stretching at wavenumber 2854 cm $^{-1}$ . Meanwhile, the asymmetrical stretching of the saturated -CH $_2$ - chain was detected at 2924 cm $^{-1}$ . The innate carbonyl group that makes up the ester bond is found at 1726 cm $^{-1}$  as carbonyl vibration of the ester bond in the polymer, along with the polymer signature signal between 1500 cm $^{-1}$  and 500 cm $^{-1}$  corresponding to work by Guo et al. (Fig. 8(a)) [56].

 $^{1}$ H NMR, confirmed the PHA structure, with five distinct peaks representing typical signals for mcl-PHA samples. A peak at 0.8 ppm was assigned to the terminal methyl group and at 1.2 ppm, represented the hydrogens from the repeated methylene groups on the monomer side chains. The peak at 1.5 ppm indicated the presence of a couple of hydrogens from a methylene group, slightly de-shielded due to its close vicinity with the ester bond containing an oxygen molecule. At 2.4–2.5 ppm, significantly more de-shielded hydrogen atoms were detected as the peaks from the methylene α-carbon of the monomer. Finally, the most de-shielded single hydrogen was detected at 5.1 ppm, representing β-chiral carbon from the monomer and directly linked to the oxygen of the ester bond (Fig. 8(b)). The integration values that predict the number of hydrogen available in the polymer derived from the analysis

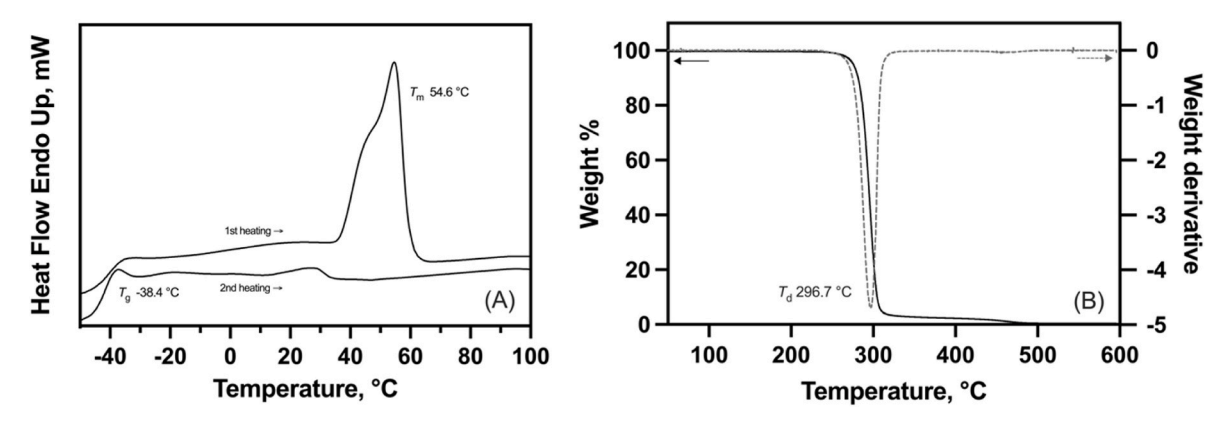
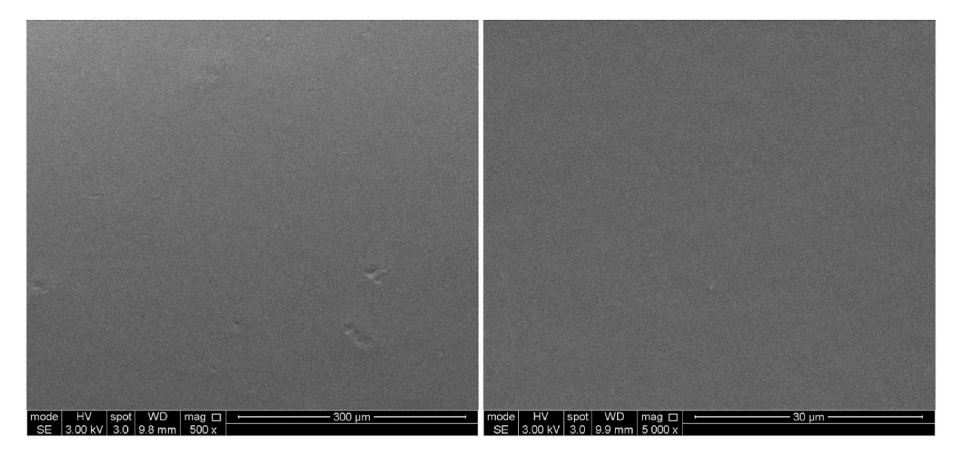
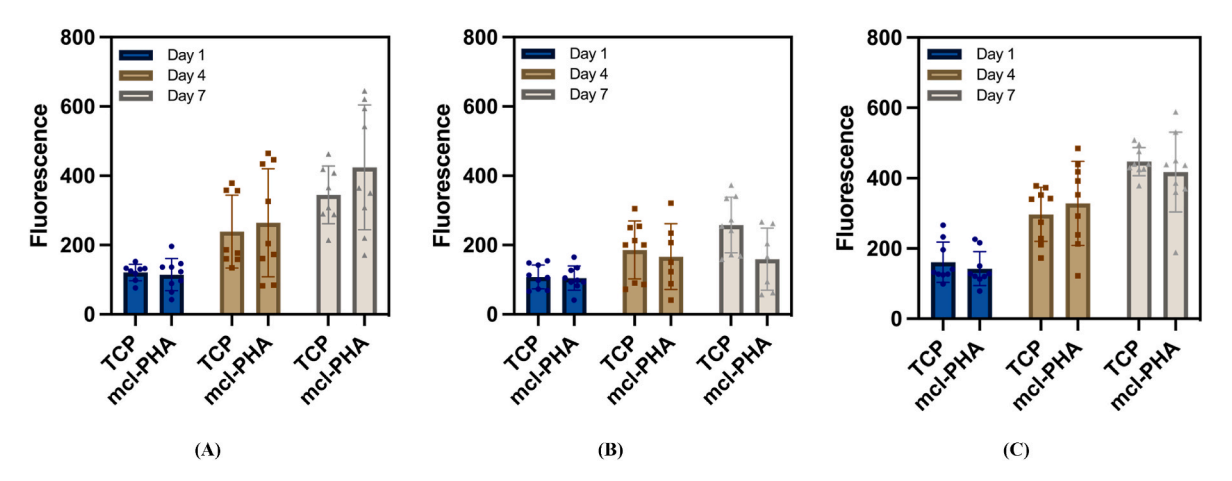


Fig. 9. Thermographs from (A) DSC analysis, and (B) TGA for mcl-PHA produced by Pseudomonas mendocina CH50.



**Fig. 10.** SEM micrograph of the surface of the mcl-PHA solvent-cast film produced by *P. mendocina* CH50 grown with glucose as the sole carbon source at two different magnifications, 500 times (*left*) and 5000 times (*right*), showing a very smooth topography.



**Fig. 11.** Resazurin reduction assay plot of the glomerular cell culture on mcl-PHA from *P. mendocina* CH50, (A) CiHP monoculture, (B) CiGEnC monoculture, and (C) CiHP and CiGEnC co-culture. The experiment setup was conducted using three independent cell passages, with triplicates of each (N = 3, n = 3), analysed with statistical assessment using 2-way ANOVA analysis, all are not significant with p > 0.5. Error bars are standard deviation.

also correspond with the monomer found from GC-MS analysis (Table S2).

These analyses ultimately demonstrated unique features of the mcl-PHA produced by  $P.\ mendocina$  CH50 with batch fermentation fed by glucose, compared to previous work (Table 2). This information summarises the varied repertoire of mcl-PHA species produced with novel attributes and distinct properties.

#### 3.2.3. Thermal, tensile and surface properties

The mcl-PHA was also subjected to differential scanning calorimetry analysis and thermogravimetric analysis to obtain the glass transition temperature ( $T_{\rm g}$ ), melting temperature ( $T_{\rm m}$ ), and degradation temperature ( $T_{\rm d}$ ).

Through DSC, the polymer was scanned twice between -70 and  $100\,^{\circ}$ C temperatures; the first scan removed the thermal history, which enabled clearer  $T_{\rm g}$  acquisition later in the second scanning. The first scan

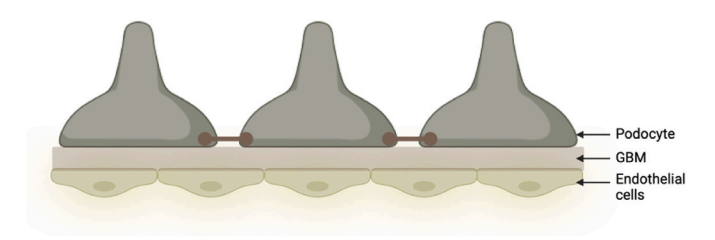


**Fig. 12.** The position of GBM which contains collagen IV in the filtration barrier of the glomerulus. The illustration is made using Biorender.com.

exhibited the  $T_{\rm m}$  as a sharp endothermal peak at 54.6 °C and a possible  $T_{\rm g}$  at around -40.9 °C. The second scan later generated a much higher resolution signal for the  $T_{\rm g}$  at -38.4 °C (Fig. 9(A)). Meanwhile, the TGA thermogram showed that the polymer started losing mass around 279.2 °C and experienced an abrupt mass drop until 308.0 °C with a maximum degradation rate at 296.7 °C based on the weight derivative curve. As the scan continued, the polymer completely degraded beyond 500 °C (Fig. 9(B)). These data exhibited typical thermal properties for thermoplastic and elastomeric polymers, especially among mcl-PHAs from *Pseudomonas* species due to the presence of a class II PHA synthase found in them, responsible for using medium chain-length monomers during PHA biosynthesis [2].

Following this, the mechanical properties of the polymer were quantified. From the DSC data, the mcl-PHA was determined to be a

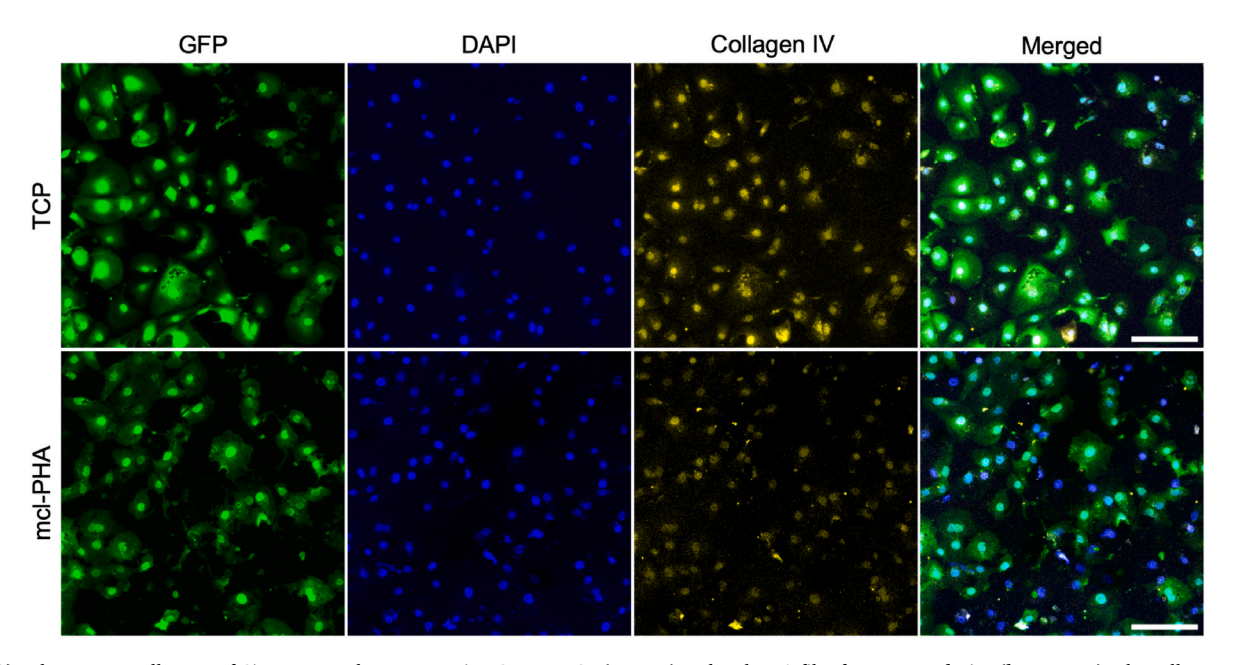


Fig. 13(A). Fluorescent cell assay of CiHP monoculture expressing GFP on TCP (top row) and mcl-PHA film from P. mendocina (bottom row). The cells were cultured over seven days under 33 °C for proliferative condition. Scale bar of 200  $\mu$ m represented in the merged images.

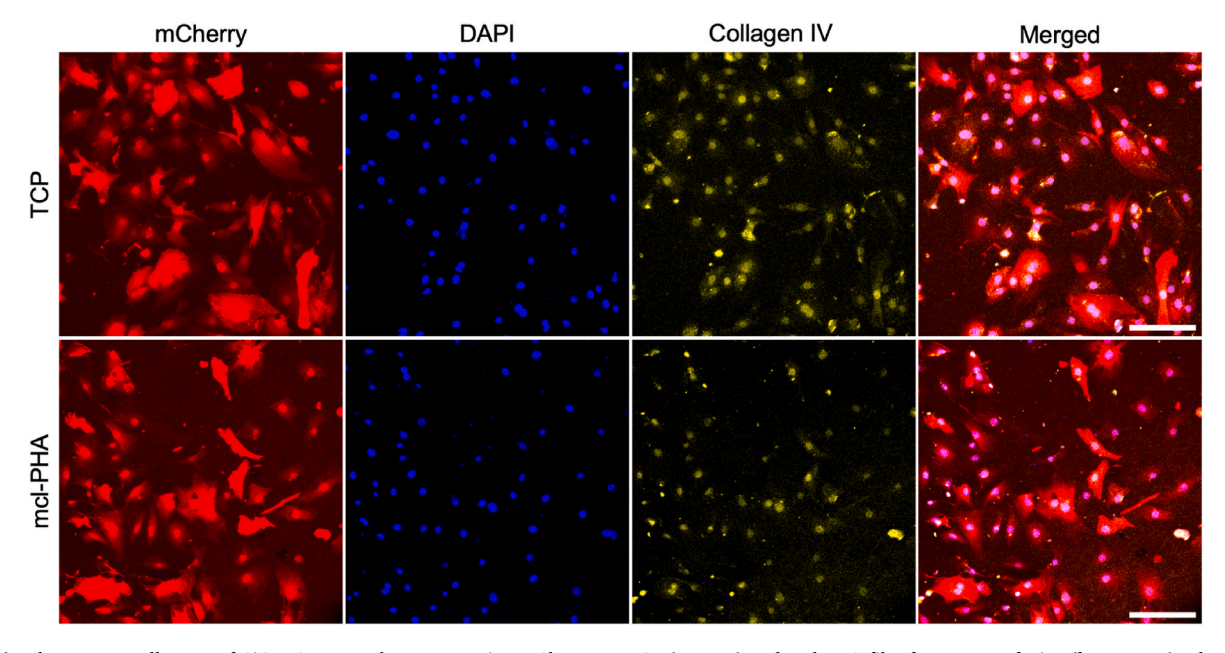


Fig. 13(B). Fluorescent cell assay of CiGEnC monoculture expressing mCherry on TCP (top row) and mcl-PHA film from P. mendocina (bottom row). The cells were cultured over seven days under 33 °C for proliferative conditions. Scale bar of 200 μm represented in the merged images.

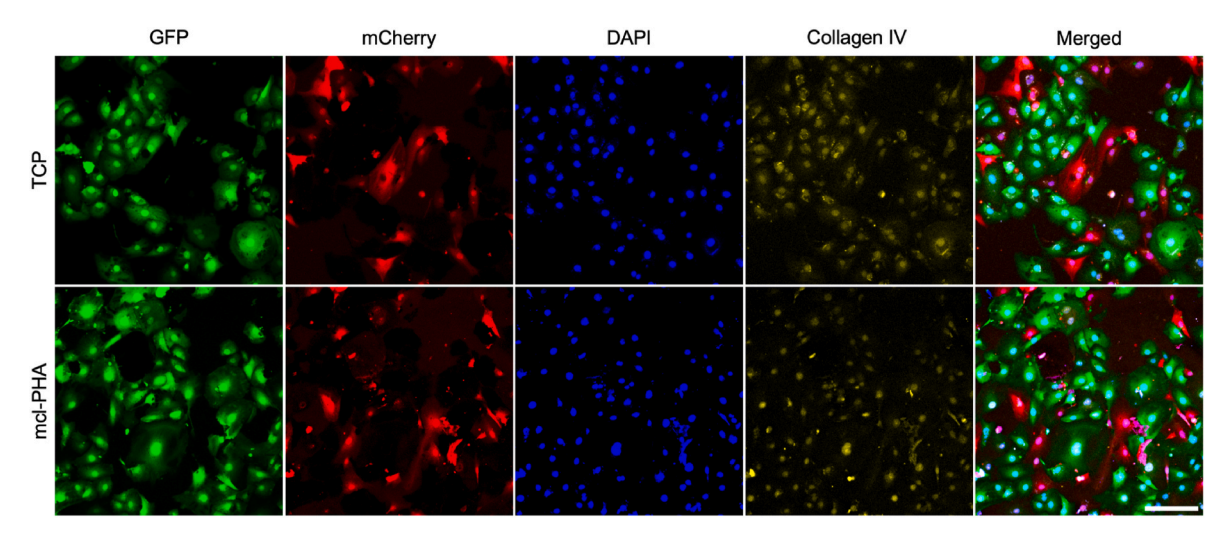


Fig. 13(C). Fluorescent cell assay of CiHP and CiGEnC co-culture on TCP (top row) and mcl-PHA film from *P. mendocina* (bottom row). The cells were cultured over seven days under 33 °C for proliferative conditions. Scale bar of 200 µm represented in the merged images.

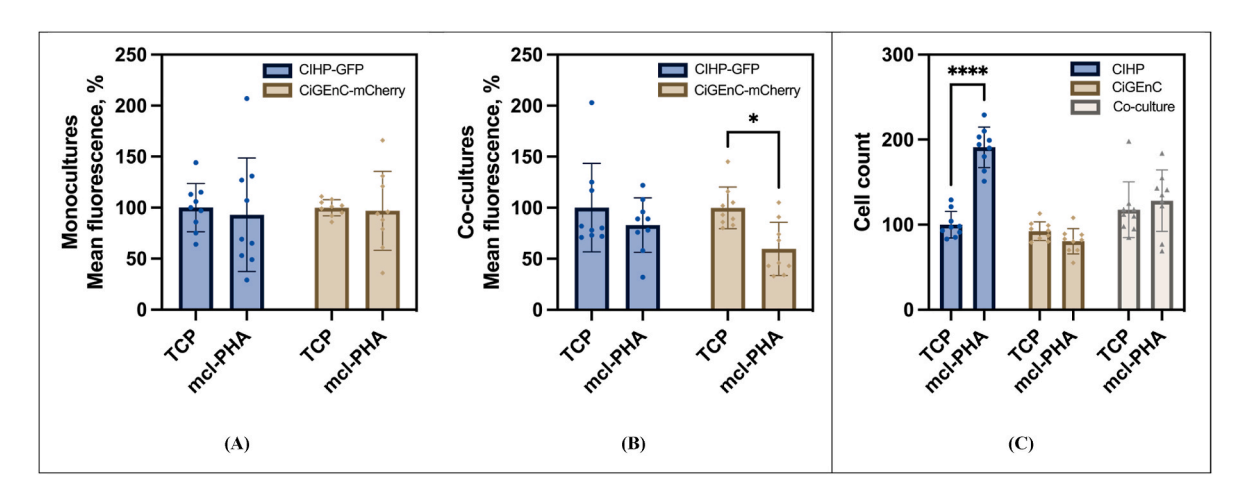


Fig. 14. Mean fluorescence plots for the fluorophore intensity of glomerular cells, (A) separate monocultures of CiHP and CiGEnC, and (B) co-culture of CiHP and CiGEnC. The CiHP and CiGEnC in (B) were cultured together, but the fluorescence was assessed separately through two different confocal channels. Meanwhile, the third plot is (C) the numerical data of cell count obtained from the DAPI nuclei stain. All data represent n=3 analysed with statistical assessment using 2-way ANOVA analysis (\* represents p<0.05, \*\* represents p<0.01, \*\*\* represents p<0.001 \*\*\* represents p<0.001; pairs without comparison are not significant with p>0.5 The cells were cultured over seven days under 33 °C for proliferative conditions. Error bars are standard deviation.

highly amorphous polymer with a degree of crystallinity,  $\Delta\chi$ , of only 5.8 %. Hence, the polymer is highly elastomeric, with  $215\pm52$  % elongation at break determined through tensile testing. The Young's modulus of the polymer was  $15\pm5$  MPa, along with ultimate tensile strength of 6  $\pm~1\,$  MPa. This is comparable to the homopolymer mcl-PHA, polyhydroxyoctanoate (PHO) produced using the same strain fed with sodium octanoate with a Young's modulus of 11.6 MPa [27], which means this material is physically and mechanically suitable for soft tissue engineering, in addition to the high 3HD monomer content by more than 70 mol%, may contribute more to its elastomeric property.

Additionally, the surface of the polymer was assessed through SEM to understand its topography, which was incredibly smooth (Fig. 10). The sample was a solvent-cast polymer film. Due to mcl-PHA being known to possess a low degree of crystallinity and an amorphous nature, the polymeric chains are relatively more mobile and tend to pack and rearrange post-volatilisation of the solvent neatly. Polymer drying *via* solvent evaporation was carried out in a controlled manner to avoid rapid drying that may introduce surface irregularities [11].

# 3.2.4. Molecular weight analysis

The weight average molecular mass,  $M_{\rm w}$ , for the mcl-PHA was

quantified to be 461 kDa, the number average molecular mass,  $M_{\rm n}$ , of 223 kDa, with a polydispersity index, PDI of 2.1. This value is hugely influenced by the type of strain used, the carbon substrate and the fermentation conditions used. The mcl-PHA produced with *P. mendocina* CH50 grown using coconut oil as a carbon source had an  $M_{\rm w}$  of 333 kDa,  $M_{\rm n}$  of 139 kDa with 2.4 PDI [11], and 496 kDa,  $M_{\rm n}$  of 282 kDa with 1.76 PDI when sodium octanoate was used as the carbon source [27]. Hence, the mcl-PHA produced in this study was on the higher side of the mcl-PHA polymer  $M_{\rm w}$  spectrum produced by *P. mendocina* CH50.

# 3.3. Glomerular cell assessment with mcl-PHA by P. mendocina CH50

The polymer performance as a potential scaffold was assessed using two established glomerular cells, conditionally immortalised human podocytes, CiHP, and conditionally immortalised glomerular endothelial cells (CiGEnC). The experimental setup involved two monocultures of the cells and a co-culture of both cells to assess the metabolic performance when cellular crosstalk occurs. The elastomeric nature of the mcl-PHA, seemed to be highly suitable for regeneration of glomerular soft tissue, hence the choice of the application.

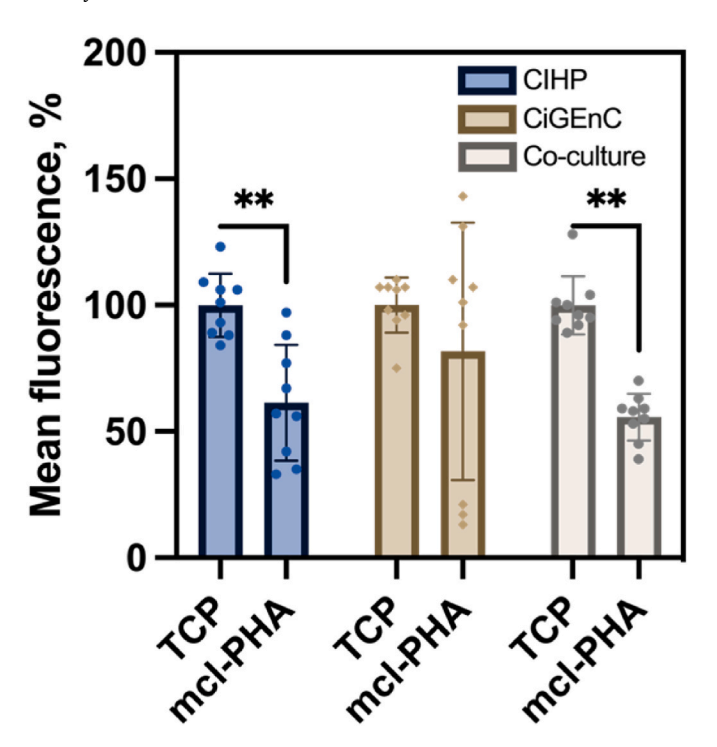


**Fig. 15.** Mean fluorescence plots for the collagen IV expression across samples, stained by immunohistochemical method. All data represent n=3 analysed with statistical assessment using 2-way ANOVA analysis (\* represents  $p<0.05, *^*$  represents  $p<0.01, *^*$  represents p<0.001 \*\*\*\* represents p<0.0001; pairs without comparison are not significant with p>0.5). The cells were cultured over seven days at 33 °C for proliferative conditions. Error bars are standard deviation.

#### 3.3.1. Metabolic activity test

The assessment for the attachment and later the proliferation of the cells was conducted by the resazurin reduction assay to assess the metabolic activity of viable cells at 33 °C which allows proliferation. Viable cells reduce the blue resazurin dye into pink resorufin, and fluorescence measurements were used to detect the change. All samples were compared with control cell culture seeded on tissue culture plastic

(TCP). On Day 1, all cultures conducted on mcl-PHAs were comparable to those on TCP without any distinct difference. The performance of CiHP and the co-culture was slightly better than TCP on Day 4, unlike the monoculture of CiGEnC, with a slightly lesser value than the TCP. Ultimately, Day 7 of proliferation revealed the best performance of CiHP on mcl-PHA, followed by the co-culture, and finally, the CiGEnC. The CiGEnC growth remained the same on the mcl-PHA between Day 4 and Day 7 as compared to TCP. Generally, all cell cultures resulted in positive proliferation across one week of incubation (Fig. 11). Two-way ANOVA statistical analysis demonstrated that the difference in proliferation between the cell culture on mcl-PHA and that on TCP as control was insignificant, with p values of Day 1 between 0.85 and 0.98, Day 4 between 0.89 and 0.97, and Day 7 between 0.11 and 0.85. This is a highly promising result, considering that glomerular cells do not generally attach and grow well on many biomaterials. For instance, in work by Tuffin et al., polyglycolic acid (PGA), as a widely used biomaterial, had to be modified with fibrin gel to make it more bioactive and allow glomerular cell attachment [61].

Both cell types are equipped with the SV40-T gene that allows proliferation at 33  $^{\circ}$ C and halts proliferation at 37  $^{\circ}$ C to induce differentiation, which allows for further assessments [35,36]. The cells grown at 33  $^{\circ}$ C were subjected to immunohistostaining to assess the production of collagen IV, which is prominent in differentiated glomerular cells. In kidney physiology, glomerular cells produce a layer of protein called the glomerular basement membrane (GBM) sandwiched by the podocytes and endothelial cells (Fig. 12). Collagen IV is one of the protein building blocks of the GBM, including others such as laminin, nidogens, and heparin sulphate proteoglycans [62].

Since both cells are over-expressing fluorophores, green fluorescent protein (GFP) for CiHP and mCherry for CiGEnC, fluorescence assay was conducted. The cells were also subjected to DAPI for nuclear staining to enable cell counting for the number of cells and immunohistochemical staining for collagen IV expression. Later, the signal intensity was measured by confocal microscopy.

#### 3.3.2. Proliferative condition

Under proliferative conditions at 33  $^{\circ}$ C incubation, the cells increase in number since the temperature is permissive for cell division. At this stage, these cell lines are undeveloped and non-functional, and further differentiation is crucial to understand proper glomerular cell behaviour

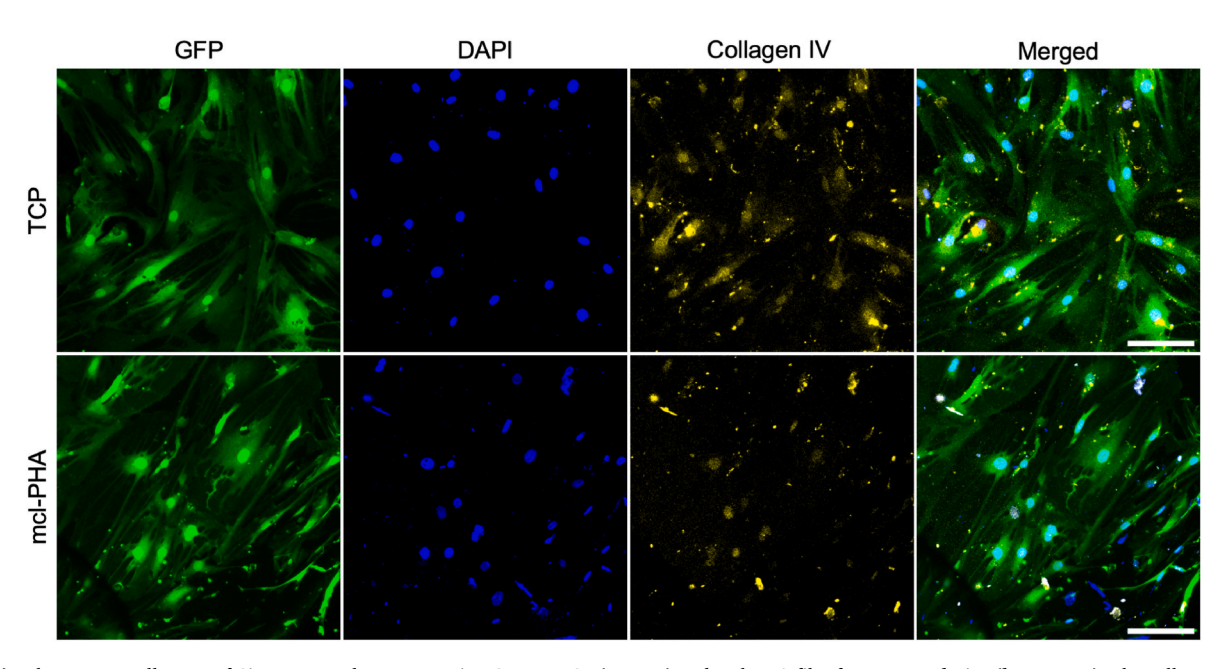
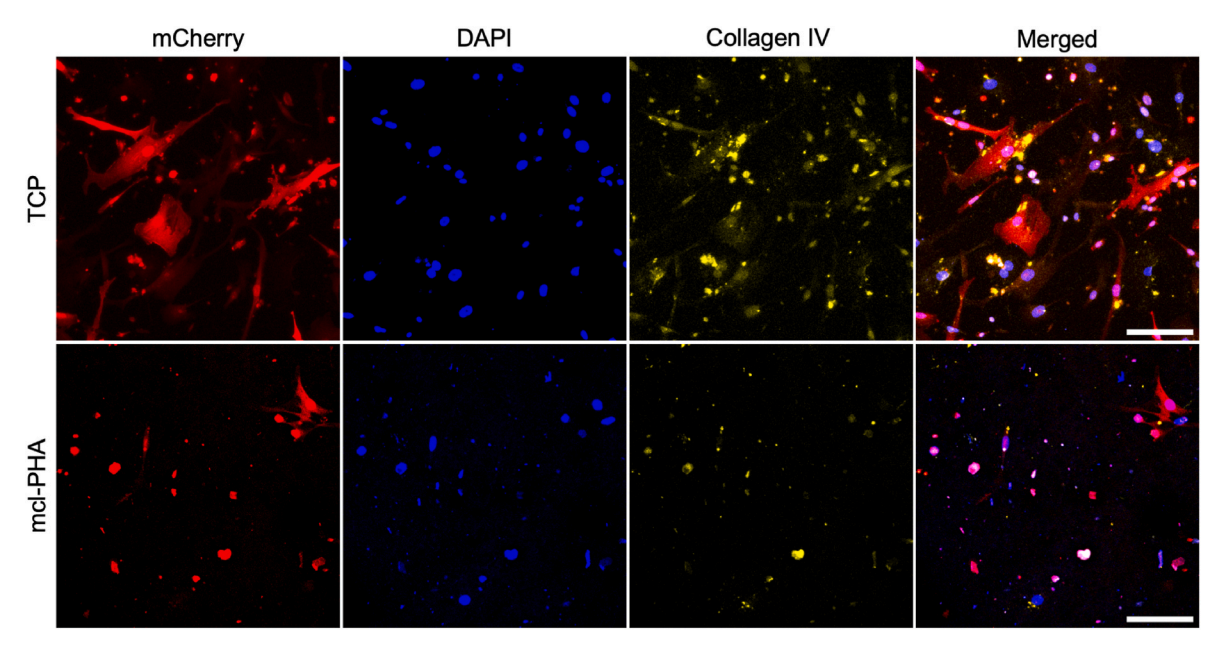


Fig. 16(A). Fluorescent cell assay of CiHP monoculture expressing GFP on TCP (top row) and mcl-PHA film from *P. mendocina* (bottom row). The cells were cultured over seven days at 33 °C for proliferative conditions and later for ten days under 37 °C for differentiative conditions (scale bar of 200 μm).



**Fig. 16(B).** Fluorescent cell assay of CiGEnC monoculture expressing mCherry on TCP (*top row*) and mcl-PHA film from *P. mendocina* (*bottom row*). The cells were cultured over seven days under 33 °C for proliferative conditions and later for ten days under 37 °C for differentiative conditions (scale bar of 200 μm).

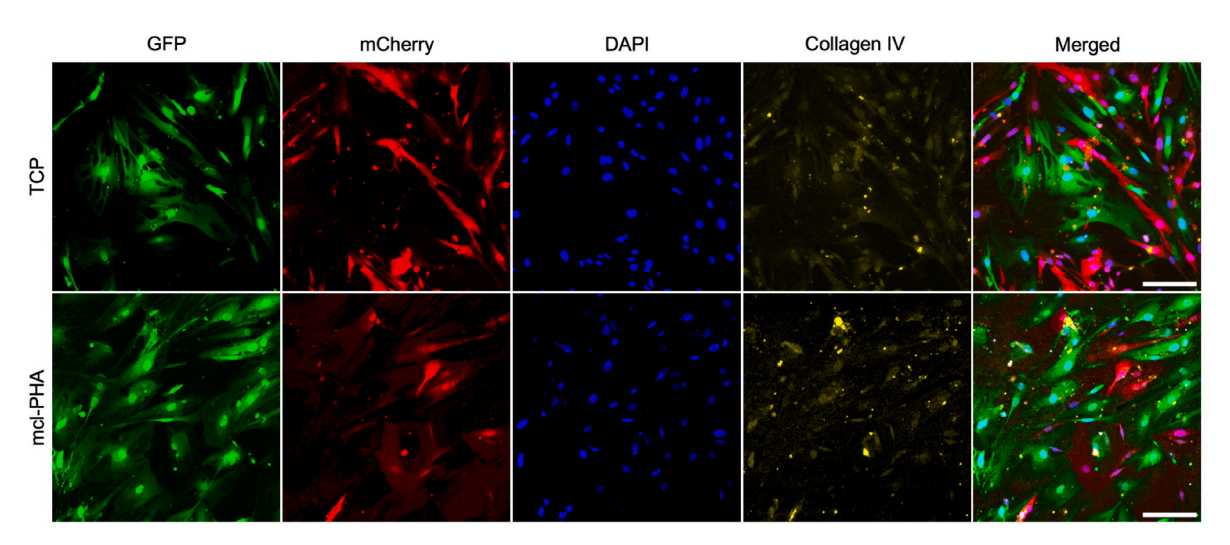


Fig. 16(C). Fluorescent cell assay of CiHP and CiGEnC co-culture on TCP (top row) and mcl-PHA film from *P. mendocina* (bottom row). The cells were cultured over seven days under 33 °C for proliferative conditions and later for ten days under 37 °C for differentiative conditions (scale bar of 200 μm).

akin to *in vivo*. Nevertheless, it is also necessary that the cells can proliferate before they are subjected to differentiative conditions, which prepares the cells to form a confluent monolayer beforehand.

Cell proliferation over seven days demonstrated visually comparable results between the TCP control and mcl-PHA film as cell culture substrate (Fig. 13). For monoculture conditions, both CiHP and CiGEnC have similar growth based on the fluorophore intensity compared to TCP (Fig. 14(A)). Meanwhile, for the co-culture, a similar observation was demonstrated for the CiHP cultured on the mcl-PHA film, which is comparable to the TCP; however, a slight decrease was observed for CiGEnC over seven days of culture (Fig. 14(B)).

The number of cells observed when cultured on TCP and mcl-PHA was quantified. The CiHP monoculture exhibited the most significant change, with 191 % growth compared to TCP per unit area when cultured across seven days on the mcl-PHA. Meanwhile, the CiGEnC monoculture exhibited no significant difference when grown on mcl-PHA compared to TCP. In contrast, the cell number on mcl-PHA for the co-culture was higher (110 %) compared to TCP (Fig. 14(C)). These

results indicate that CiHP exhibited a high proliferation on the mcl-PHA and led to better propagation in co-culture conditions with CiGEnC, either on TCP or mcl-PHA as a culture substrate.

The collagen IV expression indicated a consistent result across samples, especially for CiHP monoculture and co-culture on mcl-PHA, almost half of that observed on TCP. CiGEnC monoculture displayed statistically no significant difference; however, based on the results from the metabolic activity assessment, CiGEnC monoculture may exhibit similar metabolic performance to the CiHP monoculture and co-culture (Fig. 15).

Hence, it was confirmed that the mcl-PHA had a positive effect on the glomerular cell proliferation process and supported the production of collagen IV. Mcl-PHA is hence deemed to be a biocompatible substrate for the first step of the proliferation of the cells before differentiation.

# 3.3.3. Differentiating condition

After proliferative conditions at 33  $^{\circ}$ C incubation, the cells are thermoswitched into 37  $^{\circ}$ C incubation to allow differentiation. Both cell

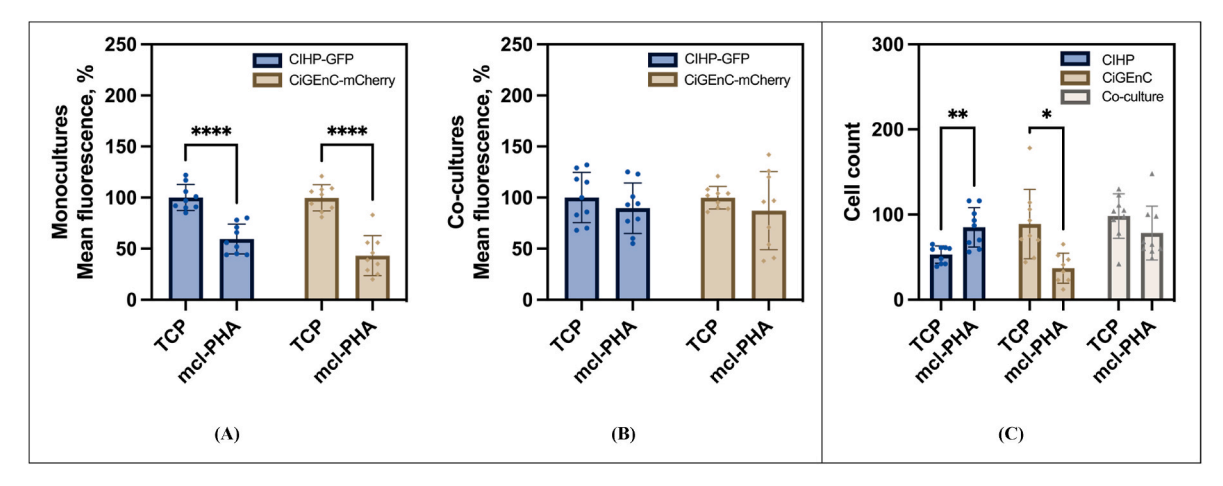
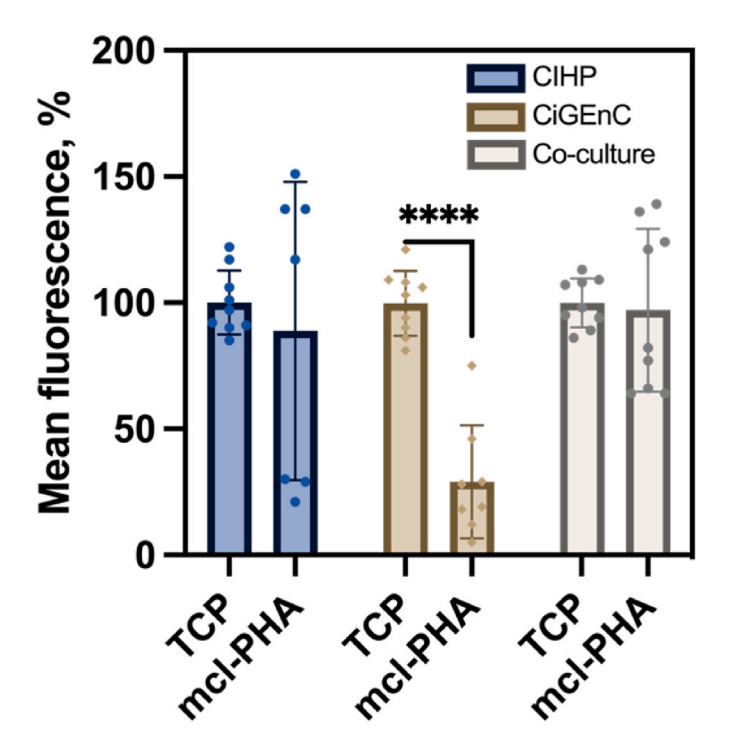


Fig. 17. Mean fluorescence plots for the fluorophore intensity of glomerular cells, (A) separate monocultures of CiHP and CiGEnC, and (B) co-culture of CiHP and CiGEnC. The CiHP and CiGEnC in (B) were cultured together, but the fluorescence was assessed separately through two different confocal channels. Meanwhile, the third plot is (C) the numerical data of cell count obtained from the DAPI nuclei stain. All data represent n=3 analysed with statistical assessment using 2-way ANOVA analysis (\* represents p<0.05, \*\* represents p<0.01, \*\*\* represents p<0.001 \*\*\* represents p<0.001; pairs without comparison are not significant with p>0.5). The cells were cultured over seven days under 33 °C for proliferative conditions and later for ten days under 37 °C for differentiative conditions. Error bars are standard deviation.



**Fig. 18.** Mean fluorescence plots for the collagen IV expression across samples, stained by immunohistochemical method. All data represent n=3 analysed with statistical assessment using 2-way ANOVA analysis (\* represents p<0.05, \*\* represents p<0.01, \*\*\* represents p<0.001 \*\*\*\* represents p<0.0001; pairs without comparison are not significant with p>0.5). The cells were cultured over seven days at 33 °C for proliferative conditions and later for ten days under 37 °C for differentiative conditions. Error bars are standard deviation.

lines contain SV40 T antigen, which halts the cell division and induces differentiation when exposed to 37 °C temperature [35,36]. When differentiated, the cells exhibit a proper physiological expression analogous to *in vivo* podocytes and glomerular endothelial cells, which embodies an accurate representation and enables further precise assessment. Like the proliferative condition, in this assessment, the cells were cultured on TCP and mcl-PHA, where TCP served as a control

culture substrate. The cells were incubated for seven days under proliferative temperature and then differentiated for ten days, hence a total of 17 days of culture.

The differentiated cell lines were morphologically different from the proliferative conditions; they are more elongated and stretched for monocultures and co-culture (Fig. 16). Unlike the proliferative conditions, both monocultures on the mcl-PHA experienced reduced cell fluorescence compared to the TCP cultures (Fig. 17(A)). The case was different for co-culture on mcl-PHA, revealing a comparable value of the mean fluorescent intensity of cells on TCP. Upon differentiation, the monocultures appear to express less fluorophores even though more cells were present. On the other hand, the co-cultures were observed to express more fluorophore, resulting in equivalent fluorescent intensity to the TCP (Fig. 17(B)).

The cell count assay was carried out as complementary information on the fluorescence intensity. CiHP exhibited lesser fluorescent intensity on mcl-PHA than on TCP; the number of cells on mcl-PHA was 60 % more than TCP. The cells on the TCP also individually appeared to be much more spread out, resulting in a higher fluorescent signal with wider cell area. In contrast, CiGEnC showed a direct relationship between the fluorophore intensity and the cell number, with 58 % fewer cells on the mcl-PHA than TCP. The co-cultures had comparable cell number between the mcl-PHA and TCP, consistent with the fluorescent assay results (Fig. 17(C)).

The collagen IV production demonstrated comparable expression between TCP and mcl-PHA for CiHP monoculture and co-cultures. CiGEnC monoculture on mcl-PHA, on the other hand, exhibited 62 % less collagen IV when compared to TCP. This is consistent with the fluorophore intensity results regarding the enhanced growth of CiHP compared to CiGEnC monocultures for the mcl-PHA substrate. Meanwhile, the co-culture on mcl-PHA again demonstrated the highly promising result of having a comparable collagen IV expression as cultured on the TCP (Fig. 18). In summary, the glomerular cells perform relatively better in a co-culture condition, upon differentiating, to sustain their growth progression possibly due to efficient cellular crosstalk between the two cell lines.

#### 4. Conclusion and Future Perspective

The mcl-PHA produced using a batch fermentation process of P. mendocina CH50 was thoroughly characterised and found to contain a range of monomers, from  $C_6$  to  $C_{14}$ , when cultured up to 48 h, making it

one of the most unique mcl-PHAs ever produced. The polymer was found to be an elastomeric polymer with thermal properties that enable its utilisation for soft tissue engineering in biomedical applications. This new biomaterial thus has a huge potential in future, and can be used to develop biomedical devices, addressing the need for regenerative medicine and, at the same time, introducing the highly important sustainability in the context of biomedical materials and devices, an aspect that PHAs as a, environmentally friendly family of polymers can offer.

In addition to the novel type of mcl-PHA produced in this study, it has also been proven to support both proliferation and differentiation of glomerular cells, especially podocytes and glomerular endothelial cells. The data obtained confirmed the suitability of the mcl-PHA as an ideal cell culture substrate, comparable to the standard TCP, that supports proliferation, differentiation and the production of the main component of GBM, collagen IV, a highly positive outcome. The differentiated culture proved that the cells performed well and were self-sustaining in enabling a proper maturation on mcl-PHA, especially the co-culture condition, demonstrating the requirement for crosstalk between the cells. The results are consistent with the need for further development of the in vitro glomerular model that necessitates the co-culture over monocultures. This study substantiates that the mcl-PHA produced in this work is an excellent sustainable material alternative in sourcing environmentally friendly bio-based materials in the biomedical area, especially in kidney tissue engineering as well as successfully served as a proof of concept and easily be used for other cell types in soft tissue engineering application.

In the future, the fermentation of P. mendocina CH50 can be further optimised to produce a higher yield of mcl-PHA. This can be done by introducing a higher initial feed concentration to the fermentation vessel or implementing the fed-batch technique [63]. Since PHAs are gaining attention on an industrial scale, especially mcl-PHAs, for their versatility, the development of a higher production scale is becoming increasingly in demand in the food industry for packaging and additives [64], also in medical sectors [65,66], given their highly biocompatible properties for biomedical application. The mcl-PHA produced in this work is an elastomeric variant of PHA with unique physical properties that make it suitable for biomedical applications. The mcl-PHA could also be blended with different types of PHAs to create polymers with even more versatile properties that can be tailored for specific applications. Furthermore, the processibility of mcl-PHAs has been well established in the Roy Lab and it is amenable to a huge array of fabrication techniques, including 3D printing, melt electrowriting, electrospinning. Hence, this work showcases a highly biocompatible and versatile polymer that has huge potential in a range of applications in the medical sector. In addition, the production of the polymer being sustainable, in this case using glucose as a renewable carbon source, provides a better solution for the future of medical materials and devices.

#### CRediT authorship contribution statement

Syed Mohammad Daniel Syed Mohamed: Writing – review & editing, Writing – original draft, Visualization, Validation, Resources, Methodology, Formal analysis, Data curation, Conceptualization. Jack Tuffin: Resources, Methodology, Investigation. Judy Watson: Resources, Methodology, Investigation. Andrea Mele: Resources, Methodology, Investigation. Annabelle Fricker: Resources, Methodology. David A. Gregory: Resources, Methodology. Elbaraa Elghazy: Methodology. Moin A. Saleem: Resources. Simon C. Satchell: Resources. Gavin I. Welsh: Writing – review & editing, Validation, Supervision, Project administration, Investigation, Data curation, Conceptualization. Ipsita Roy: Writing – review & editing, Supervision, Project administration, Investigation, Funding acquisition, Data curation, Conceptualization.

#### Data availability statement

Data for this paper are available at the University of Sheffield data repository, ORDA, at https://doi.org/10.15131/shef.data.27210891.

#### Declaration of competing interest

The authors declare that they have no known competing financial interests or personal relationships that could have appeared to influence the work reported in this paper.

#### Acknowledgement

The author acknowledges the grants granted by Engineering and Physical Sciences Research Council (EPSRC), number EP/V012126/1, EP/X021440/1 and EP/X026108/1, as well as PhD scholarship, *Program Pelajar Cemerlang*, granted to the first author by the Government of Malaysia through Malaysia Public Services Department. The authors would also like to express the utmost appreciation to Dr Katy Jepson and Alan Leard for their support at Wolfson Bioimaging Facility, University of Bristol, Professor Mike Williamson from the School of Bioscience, University of Sheffield, for his wisdom and insight in interpreting NMR spectra, and Dr Oday Hussain for his assistance for basic characterisation of the polymer at Royce Discovery Centre, University of Sheffield—special thanks to Dr Enes Durgut and Soponvit Larpnimitchai for their kind help in acquiring the SEM images.

#### Appendix A. Supplementary data

Supplementary data to this article can be found online at https://doi. org/10.1016/j.mtbio.2025.101932.

#### Data availability

Data for this paper are available at the University of Sheffield data repository, ORDA, at https://doi.org/10.15131/shef.data.27210891.

#### References

- Xu, T.; Huang, X.-Y.; Dao, J.-W.; Xiao, D.; Wei, D.-X. Synthetic biology for medical biomaterials. Interdisciplinary Medicine n/a (n/a), e20240087.
- [2] J. Mozejko-Ciesielska, K. Szacherska, P. Marciniak, Pseudomonas species as producers of eco-friendly polyhydroxyalkanoates, J. Polym. Environ. 27 (6) (2019) 1151–1166
- [3] J.-Y. Chen, T. Liu, Z. Zheng, J.-C. Chen, G.-Q. Chen, Polyhydroxyalkanoate synthases PhaC1 and PhaC2 from Pseudomonas stutzeri 1317 had different substrate specificities, Fems Microbiol Lett 234 (2) (2006) 231–237.
- [4] D. Jendrossek, Carbonosomes, in: D. Jendrossek (Ed.), Bacterial Organelles and Organelle-like Inclusions, Springer International Publishing, 2020, pp. 243–275.
- [5] D. Jendrossek, D. Pfeiffer, New insights in the formation of polyhydroxyalkanoate granules (carbonosomes) and novel functions of poly(3-hydroxybutyrate), Environ. Microbiol. 16 (8) (2014) 2357–2373.
- [6] A. Prieto, I.F. Escapa, V. Martínez, N. Dinjaski, C. Herencias, F. de la Peña, N. Tarazona, O. Revelles, A holistic view of polyhydroxyalkanoate metabolism in Pseudomonas putida, Environ. Microbiol. 18 (2) (2016) 341–357.
- [7] B. Witholt, B. Kessler, Perspectives of medium chain length poly (hydroxyalkanoates), a versatile set of bacterial bioplastics, Curr Opin Biotech 10 (3) (1999) 279–285.
- [8] M.S.d.F. Diniz, M.M. Mourão, L.P. Xavier, A.V. Santos, Recent Biotechnological applications of polyhydroxyalkanoates (PHA) in the biomedical Sector—a review, Polymers-Basel 15 (2023) 4405.
- [9] M.H. Al-Zaidi, W.H. Al-Tamimi, A.A. Saleh, Characterization and Antibacterial Activity of the Natural Biopolymer Extracted from Pseudomonas aeruginosa, 2023.
- [10] J. Lalucat, A. Bennasar, R. Bosch, E. García-Valdés, N.J. Palleroni, Biology of Pseudomonas stutzeri, Microbiol Mol Biol R 70 (2) (2006) 510–547.
- [11] P. Basnett, E. Marcello, B. Lukasiewicz, B. Panchal, R. Nigmatullin, J. Knowles, I. Roy, Biosynthesis and characterization of a novel, biocompatible medium chain length polyhydroxyalkanoate by Pseudomonas mendocina CH50 using coconut oil as the carbon source. J. Mater. Sci. Mater. Med. 29 (179) (2018).
- [12] W. Chanasit, B. Hodgson, K. Sudesh, K. Umsakul, Efficient production of polyhydroxyalkanoates (PHAs) from Pseudomonas mendocina PSU using a biodiesel liquid waste (BLW) as the sole carbon source, Biosci. Biotechnol. Biochem. 80 (7) (2016) 1440–1450.

[13] M. Kacanski, F. Stelzer, M. Walsh, S. Kenny, K. O'Connor, M. Neureiter, Pilot-scale production of mcl-PHA by Pseudomonas citronellolis using acetic acid as the sole carbon source, New Biotechnol 78 (2023) 68–75.

- [14] P. Unrean, S.C. Napathorn, K.L. Tee, T.S. Wong, V. Champreda, Lignin to polyhydroxyalkanoate bioprocessing by novel strain of Pseudomonas monteilii, Biomass Conversion and Biorefinery 13 (6) (2023) 4651–4657.
- [15] F. Cerrone, B. Zhou, A. Mouren, L. Avérous, S. Conroy, J.C. Simpson, K. E. O'Connor, T. Narancic, Pseudomonas umsongensis GO16 as a platform for the in vivo synthesis of short and medium chain length polyhydroxyalkanoate blends, Bioresour. Technol. 387 (2023) 129668.
- [16] S. Tienda, J.A. Gutiérrez-Barranquero, I. Padilla-Roji, E. Arrebola, A. de Vicente, F. M. Cazorla, Polyhydroxyalkanoate production by the plant beneficial rhizobacterium Pseudomonas chlororaphis PCL1606 influences survival and rhizospheric performance, Microbiol. Res. 278 (2024) 127527.
- [17] N. Mohanan, M.C.-H. Wong, N. Budisa, D.B. Levin, Polymer-degrading enzymes of Pseudomonas chloroaphis PA23 display broad substrate preferences, Int. J. Mol. Sci. 24 (5) (2023) 4501.
- [18] W. He, W. Tian, G. Zhang, G.-Q. Chen, Z. Zhang, Production of novel polyhydroxyalkanoates by Pseudomonas stutzeri 1317 from glucose and soybean oil, Fems Microbiol Lett 169 (1) (1998) 45–49.
- [19] E.R. Olivera, D. Carnicero, R. Jodra, B. Miñambres, B. García, G.A. Abraham, A. Gallardo, J.S. Román, J.L. García, G. Naharro, et al., Genetically engineered Pseudomonas: a factory of new bioplastics with broad applications, Environ. Microbiol. 3 (10) (2001) 612–618.
- [20] M. Kacanski, F. Stelzer, M. Walsh, S. Kenny, K. O'Connor, M. Neureiter, Pilot-scale production of mcl-PHA by Pseudomonas citronellolis using acetic acid as the sole carbon source, N. Biotech. 78 (2023) 68–75.
- [21] S. Follonier, R. Riesen, M. Zinn, Pilot-scale production of functionalized mcl-PHA from grape pomace supplemented with fatty acids, Chem. Biochem. Eng. Q. 29 (2) (2015) 113–121.
- [22] Y. Elbahloul, A. Steinbüchel, Large-scale production of poly(3-hydroxyoctanoic acid) by *Pseudomonas putida* GPo1 and a simplified downstream process, Appl. Environ. Microbiol. 75 (3) (2009) 643–651.
- [23] A.B. Kroumova, G.J. Wagner, H.M. Davies, Biochemical observations on medium-chain-length polyhydroxyalkanoate biosynthesis and accumulation in Pseudomonas mendocina, Arch. Biochem. Biophys. 405 (1) (2002) 95–103.
- [24] W. Tian, K. Hong, G.-Q. Chen, Q. Wu, R.-q. Zhang, W. Huang, Production of polyesters consisting of medium chain length 3-hydroxyalkanoic acids by Pseudomonas mendocina 0806 from various carbon sources, Antonie Leeuwenhoek 77 (1) (2000) 31–36.
- [25] A. Röttig, A. Steinbüchel, Acyltransferases in bacteria, Microbiol Mol Biol R 77 (2) (2013) 277–321.
- [26] G. Zhang, Q. Wu, W. Tian, K. Hong, S. Sun, R. Zhang, G. Chen, Production of medium chain length polyhydroxyalkanoates by Pseudomonas mendocina 0806 from related and unrelated carbon sources, Tsinghua Sci. Technol. 4 (3) (1999) 1535–1538.
- [27] R. Rai, D.M. Yunos, A.R. Boccaccini, J.C. Knowles, I.A. Barker, S.M. Howdle, G. D. Tredwell, T. Keshavarz, I. Roy, Poly-3-hydroxyoctanoate P(3HO), a medium chain length polyhydroxyalkanoate homopolymer from Pseudomonas mendocina, Biomacromolecules 12 (6) (2011) 2126–2136.
- [28] F. Zhao, F. He, X. Liu, J. Shi, J. Liang, S. Wang, C. Yang, R. Liu, Metabolic engineering of Pseudomonas mendocina NK-01 for enhanced production of medium-chain-length polyhydroxyalkanoates with enriched content of the dominant monomer, Int. J. Biol. Macromol. 154 (2020) 1596–1605.
- [29] F. Zhao, T. Gong, X. Liu, X. Fan, R. Huang, T. Ma, S. Wang, W. Gao, C. Yang, Morphology engineering for enhanced production of medium-chain-length polyhydroxyalkanoates in Pseudomonas mendocina NK-01, Appl Microbiol Biot 103 (4) (2019) 1713–1724.
- [30] N. Owji, N. Mandakhbayar, D.A. Gregory, E. Marcello, H.W. Kim, I. Roy, J. C. Knowles, Mussel inspired Chemistry and bacteria derived polymers for oral mucosal Adhesion and drug delivery, Front. Bioeng. Biotechnol. 9 (2021) 663764.
- [31] D.-X. Wei, J.-W. Dao, G.-Q. Chen, A micro-ark for cells: highly open porous polyhydroxyalkanoate microspheres as injectable scaffolds for tissue regeneration, Adv. Mater. 30 (31) (2018) 1802273.
- [32] D.-X. Wei, D. Cai, Y. Tan, K. Liu, J.-W. Dao, X. Li, A. Muheremu, Poly(3-hydroxybutyrate-co-3-hydroxyvalerate-co-3-hydroxyhexanoate)-based microspheres as a sustained platform for Huperzine A delivery for alzheimer's disease therapy, Int. J. Biol. Macromol. 282 (2024) 136582.
- [33] Y.-W. Ding, Y. Li, Z.-W. Zhang, J.-W. Dao, D.-X. Wei, Hydrogel forming microneedles loaded with VEGF and Ritlecitinib/polyhydroxyalkanoates nanoparticles for mini-invasive androgenetic alopecia treatment, Bioact. Mater. 38 (2024) 95–108.
- [34] X.-Y. Huang, X.-X. Zhou, H. Yang, T. Xu, J.-W. Dao, L. Bian, D.-X. Wei, Directed osteogenic differentiation of human bone marrow mesenchymal stem cells via sustained release of BMP4 from PBVHx-based nanoparticles, Int. J. Biol. Macromol. 265 (2024) 130649.
- [35] M.A. Saleem, M.J. O'Hare, J. Reiser, R.J. Coward, C.D. Inward, T. Farren, C. Y. Xing, L. Ni, P.W. Mathieson, P. Mundel, A conditionally immortalized human podocyte cell line demonstrating Nephrin and Podocin expression, J. Am. Soc. Nephrol. 13 (3) (2002) 630–638.
- [36] S.C. Satchell, C.H. Tasman, A. Singh, L. Ni, J. Geelen, C.J. von Ruhland, M. J. O'Hare, M.A. Saleem, L.P. van den Heuvel, P.W. Mathieson, Conditionally immortalized human glomerular endothelial cells expressing fenestrations in response to VEGF, Kidney Int. 69 (9) (2006) 1633–1640.
- [37] R. Rai, J.A. Roether, J.C. Knowles, N. Mordan, V. Salih, I.C. Locke, M.P. Gordge, A. McCormick, D. Mohn, W.J. Stark, et al., Highly elastomeric poly(3-

- hydroxyoctanoate) based natural polymer composite for enhanced keratinocyte regeneration, International Journal of Polymeric Materials and Polymeric Biomaterials 66 (7) (2017) 326–335.
- [38] P. Basnett, B. Lukasiewicz, E. Marcello, H.K. Gura, J.C. Knowles, I. Roy, Production of a novel medium chain length poly(3-hydroxyalkanoate) using unprocessed biodiesel waste and its evaluation as a tissue engineering scaffold, Microb. Biotechnol. 10 (6) (2017) 1384–1399.
- [39] P. Basnett, E. Marcello, B. Lukasiewicz, R. Nigmatullin, A. Paxinou, M.H. Ahmad, B. Gurumayum, I. Roy, Antimicrobial materials with Lime oil and a poly(3hydroxyalkanoate) produced via Valorisation of sugar Cane Molasses, J. Funct. Biomater. 11 (2) (2020).
- [40] A.V. Bagdadi, M. Safari, P. Dubey, P. Basnett, P. Sofokleous, E. Humphrey, I. Locke, M. Edirisinghe, C. Terracciano, A.R. Boccaccini, et al., Poly(3-hydroxyoctanoate), a promising new material for cardiac tissue engineering, J. Tissue Eng. Regen. Med. 12 (1) (2018) e495–e512.
- [41] Z. Xu, X. Li, N. Hao, C. Pan, L. de la torre, A. Ahamed, J.H. Miller, A.J. Ragauskas, J. Yuan, B. Yang, Kinetic understanding of nitrogen supply condition on biosynthesis of polyhydroxyalkanoate from benzoate by Pseudomonas putida KT2440, Bioresour. Technol. 273 (2019) 538–544.
- [42] R. Davis, R. Kataria, F. Cerrone, T. Woods, S. Kenny, A. O'Donovan, M. Guzik, H. Shaikh, G. Duane, V.K. Gupta, et al., Conversion of grass biomass into fermentable sugars and its utilization for medium chain length polyhydroxyalkanoate (mcl-PHA) production by Pseudomonas strains, Bioresour. Technol. 150 (2013) 202–209.
- [43] S.M.D.S. Mohamed, K.A. Ishak, M.S.M. Annuar, T.S. Velayutham, Synthesis and characterization of methyl acrylate-copolymerized medium-chain-length poly-3hydroxyalkanoates, J. Polym. Environ. 29 (2021) 3004–3014.
- [44] M. Syed, S. Annuar, T. Heidelberg, N. Ansari, N. Ismail, Porous amphiphilic biogel from facile chemo-biosynthetic route, J. Serb. Chem. Soc. (00) (2019) 101, 101.
- [45] J. Tuffin, M. Burke, T. Richardson, T. Johnson, M.A. Saleem, S. Satchell, G.I. Welsh, A. Perriman, A composite hydrogel scaffold permits self-organization and matrix deposition by Cocultured human glomerular cells, Adv Healthc Mater 8 (17) (2019) 1–11.
- [46] A. Tomar, P. Uysal-Onganer, P. Basnett, U. Pati, I. Roy, 3D disease Modelling of hard and soft cancer using PHA-based scaffolds, Cancers (Basel) 14 (14) (2022).
- [47] R.J. Sánchez, J. Schripsema, L.F. da Silva, M.K. Taciro, J.G.C. Pradella, J.G. C. Gomez, Medium-chain-length polyhydroxyalkanoic acids (PHAmcl) produced by Pseudomonas putida IPT 046 from renewable sources, Eur. Polym. J. 39 (7) (2003) 1385–1394.
- [48] G.-Q. Chen, Plastics completely Synthesized by bacteria: polyhydroxyalkanoates, in: G.G.-Q. Chen (Ed.), Plastics from Bacteria: Natural Functions and Applications, Springer Berlin Heidelberg, 2010, pp. 17–37.
- [49] P. Basnett, E. Marcello, B. Lukasiewicz, B. Panchal, R. Nigmatullin, J.C. Knowles, I. Roy, Biosynthesis and characterization of a novel, biocompatible medium chain length polyhydroxyalkanoate by Pseudomonas mendocina CH50 using coconut oil as the carbon source, J. Mater. Sci. Mater. Med. 29 (12) (2018).
- [50] R.D. Ashby, T.A. Foglia, Poly(hydroxyalkanoate) biosynthesis from triglyceride substrates, Appl Microbiol Biot 49 (4) (1998) 431–437.
- [51] J. Lu, R.C. Tappel, C.T. Nomura, Mini-review: biosynthesis of poly (hydroxyalkanoates), Polym. Rev. 49 (3) (2009) 226–248.
- [52] S. Zher Neoh, M. Fey Chek, H. Tiang Tan, J.A. Linares-Pastén, A. Nandakumar, T. Hakoshima, K. Sudesh, Polyhydroxyalkanoate synthase (PhaC): the key enzyme for biopolyester synthesis, Current Research in Biotechnology 4 (2022) 87–101.
- [53] S. Liu, T. Narancic, J.-L. Tham, K.E. O'Connor, β-oxidation–polyhydroxyalkanoates synthesis relationship in Pseudomonas putida KT2440 revisited, Appl Microbiol Biot 107 (5) (2023) 1863–1874.
- [54] W. Guo, C. Song, M. Kong, W. Geng, Y. Wang, S. Wang, Simultaneous production and characterization of medium-chain-length polyhydroxyalkanoates and alginate oligosaccharides by Pseudomonas mendocina NK-01, Appl. Microbiol. Biotechnol. 92 (4) (2011) 791–801.
- [55] K. Hong, G.Q. Chen, P.H. Yu, G. Zhang, Y. Liu, H. Chua, Effect of C:N molar ratio on monomer composition of polyhydroxyalkanoates produced by Pseudomonas mendocina 0806 and Pseudomonas pseudoalkaligenus YS1, Appl. Biochem. Biotechnol. 84–86 (2000) 971–980.
- [56] W. Guo, J. Duan, W. Geng, J. Feng, S. Wang, C. Song, Comparison of medium-chain-length polyhydroxyalkanoates synthases from Pseudomonas mendocina NK-01 with the same substrate specificity, Microbiol. Res. 168 (4) (2013) 231–237.
- [57] D.Y. Kim, H.W. Kim, M.G. Chung, Y.H. Rhee, Biosynthesis, modification, and biodegradation of bacterial medium-chain-length polyhydroxyalkanoates, J. Microbiol. 45 (2) (2007) 87–97.
- [58] M. Nitschke, S.G.V.A.O. Costa, J. Contiero, Rhamnolipids and PHAs: Recent reports on Pseudomonas-derived molecules of increasing industrial interest, Process Biochem. 46 (3) (2011) 621–630.
- [59] O. Rojas-Rosas, J. Villafaña-Rojas, F.A. López-Dellamary, J. Nungaray-Arellano, O. González-Reynoso, Production and characterization of polyhydroxyalkanoates in Pseudomonas aeruginosa ATCC 9027 from glucose, an unrelated carbon source, Can. J. Microbiol. 53 (7) (2007) 840–851.
- [60] C. Simon-Colin, C. Gouin, P. Lemechko, S. Schmitt, A. Senant, N. Kervarec, J. Guezennec, Biosynthesis and characterization of polyhydroxyalkanoates by Pseudomonas guezennei from alkanoates and glucose, Int. J. Biol. Macromol. 51 (5) (2012) 1063–1069.
- [61] J. Tuffin, M. Chesor, V. Kuzmuk, T. Johnson, S.C. Satchell, G.I. Welsh, M. A. Saleem, GlomSpheres as a 3D co-culture spheroid model of the kidney glomerulus for rapid drug-screening, Commun. Biol. 4 (1) (2021) 1351.
- [62] R.W. Naylor, M.R.P.T. Morais, R. Lennon, Complexities of the glomerular basement membrane, Nat. Rev. Nephrol. 17 (2) (2021) 112–127.

- [63] J.M. Borrero-de Acuña, M. Rohde, C. Saldias, I. Poblete-Castro, Fed-batch mcl-polyhydroxyalkanoates production in Pseudomonas putida KT2440 and ΔphaZ mutant on biodiesel-derived Crude Glycerol, Front. Bioeng. Biotechnol. 9 (2021). Brief Research Report.
- [64] S.S. Selvi, E. Eminagic, M.Y. Kandur, E. Ozcan, C. Kasavi, E.T. Oner, Research and production of microbial polymers for food industry, in: Bioprocessing for Biomolecules Production, 2019, pp. 211–238.
- [65] C.J. Brigham, A.J. Sinskey, Application of polyhydroxyalkanoates in the medical industry, Int. J. Biotechnol. Wellness Ind. 1 (1) (2012) 53–60.
- [66] Z.-W. Ren, Z.-Y. Wang, Y.-W. Ding, J.-W. Dao, H.-R. Li, X. Ma, X.-Y. Yang, Z.-Q. Zhou, J.-X. Liu, C.-H. Mi, et al., Polyhydroxyalkanoates: the natural biopolyester for future medical innovations, Biomater. Sci. 11 (18) (2023) 6013–6034, https://doi.org/10.1039/D3BM01043K.